Title

Development of a training atlas for improving the validity of landmark location in three dimensional x-ray cephalometry

Author

San Vicente, Amarilis,

Publication Date

1984

Peer reviewed|Thesis/dissertation

Development of a training atlas for improving the Validity of Landmark Location in Three Dimensional X-Ray Cephalometry.

by

AMARILIS SAN VICENTE

THESIS

Submitted in partial satisfaction of the requirements for the degree of

MASTER OF SCIENCE

in

ORAL BIOLOGY

in the

GRADUATE DIVISION

of the

UNIVERSITY OF CALIFORNIA

San Francisco

Date University Librarian

JUN 17 1984

Degree Conferred: . . . . . .

Acknowledgements

This work was made possible by the cooperation of a number of people. I wish first to express my deep gratitude to my professor and advisor Dr. Sheldon Baumrind who motivated me to undertake this thesis. I also wish to thank Dr. John Greenspan for his confidence in me and to thank all the other faculty and staff personnel of the Department of Oral Biology and of the Department of Growth and Development for their cooperation.

I am indebted to Leslie O'Keeffe and Randy Noble for their expert assistance in typing and editing the manuscript.

Finally, I wish to express my appreciation to my sponsor Fundacion Gran Mariscal de Ayacucho (Venezuela) for supporting me during my years of study.

TABLE OF CONTENTS

Introduction

Biostereometrics, the science of measuring biological forms in space, has a long and venerable history (1,2). During the Italian Renaissance, graphic artists were probably among the first to explore formal methods for reproducing the human form in a natural and realistic way. They were confronted with the problem of obtaining relevant information about three dimensional objects in the real world and of successfully translating that three dimensional information into a two dimensional painting or a bas-relief sculpture. Da Vinci, Alberti, Michaelangelo and Giberti were gifted mathematicians and were able to apply geometrical principles to their tasks. Alberti's recognition of the unique power of analytic coordinate systems to describe human body form antedates the recent growth of analytical methods in topographic mapping by almost five hundred years. In 1440, Alberti published his book, Della Statua for use by sculptors in the application of geometric surveying principles to the depiction of the human body (3).

The principles of biostereometrics and perspective thus established were commonly used by architects, engineers and artists in the later Renaissance. No further significant conceptual contributions to the field were made until 1832, the date which marked the invention of the stereoscope by Charles Wheatstone (4). The principle of the stereoscope depends on presenting two drawings made from slightly dif-

ferent viewpoints, each to a single eye. If the drawings are properly configured, it is possible to "fool" the eye in such a way as to cause the viewer to assemble the two images cerebrally to form a single three dimensional image (Fig. 1) (5). Shortly after Wheatstone's discovery, photography became practical and in a few years stereo cameras had been devised and were being used for qualitative topographic documentation. Physicians, topographers and engineers found stereo photography particularly useful in various documentation aspects of their respective fields. Quantitative stereophotogrammetry developed from these earlier applications and has been the main method for aerial cartography ever since.

Current craniofacial biologists and investigators owe a great deal to the contributions of the early stereophotogrammetrists. But their debt also extends to members of another and quite different discipline, the physical anthropologists. Physical anthropology is a branch of anthropology, the study of human physical and cultural diversity. Physical anthropology first achieved its name and scientific status by measuring the human body as an aid to the study of human evolution and biological variation (6). As long ago as 1543, the anatomist Vesalius attempted to define associations between skull type and ethnic origin (7). Different anthropometric measurements have been devised and used by researchers in this field and have been applied to both living subjects and skeletal remains.

Probably the most significant application of anthropometry is in the study of human growth. By the late 1800's, physical anthropologists had already established sets of anatomical landmarks known in their field as anthropological landmarks. Nasion, Pasion, Pogonion, Frankfort Plane and Camper's Plane are among the anthropometric terms whose definitions were established during this period. In 1895, a meeting of physical anthropologists at Frankfurt devised a set of standards for measuring these landmarks on dried specimens. Craniofacial investigators still utilize many of the definitions for anatomical structures which were established by physical anthropologists at that meeting. In the same year, the discovery of the x-ray by Roentgen made it possible to observe internal structures in living human subjects. Early x-ray machines were relatively crude, represented a considerable electrical hazard and had relatively poor imaging characteristics. Although the first example of x-ray stereoscopy antedated 1900 (8), the image quality of most early roentgenographs was sufficiently poor so that quantitative measurement was impractical. However, technological improvements in x-ray image quality proceeded quite rapidly after the first World War and by 1925 it became practical for Broadbent in the United States and Hofrath in Germany to make systematic attempts to obtain three dimensional x-ray information from paired x-ray films. Both these workers rejected the stereoscopic method of Wheatstone and chose instead to attempt to gather informa-

together the perspective points of the two films are. If one desires to identify both unambiguous metallic markers and ambiguous anatomical structures on the same film pair, then one must seek some optimal angle of displacement between the two x-ray locations which is substantially greater than zero, but considerably less than ninety degrees. Based on these concepts, Baumrind and co-workers (12,13,14), have attempted to construct a three dimensional roentgenographic stereo cephalometric system in which the two images are projected on coplanar films from x-ray emitter locations sited approximately twenty degrees apart. (Fig.3) In supporting the rationale of his method, Baumrind states that in the coplanar solution, "The distance between the two tube positions has been reduced, greatly simplifying the problem of identifying the same landmark on both films and allowing one of the projections of each pair to be a standard one. The reduction of the angle between the rays from the two tubes to any given landmark in the object results in a reduction in the strength of the mathematical solution. However the improved reliability in landmark identification between films more than makes up for this degradation in mathematical power, leaving this the optimal solution for most problems involving identification of anatomical landmarks."

Some introductory information on the mechanism of stereoscopic distance ranging seems in order. The normal processes of the human binocular vision constitute an

excellent model (Fig. 4). When a person views a point at a distance, the eyes rotate toward that point. If an imaginary line is drawn from the lens of each eye through the point observed, the two lines will converge at the point. The angle formed by the intersection of these two lines is called the parallactic angle of the point. Points viewed from different distances have different parallactic angles. The brain interprets these differences in parallactic angle as differences in distance. The further away a point is from the viewer the smaller the parallactic angle becomes. Because the human eyes are situated so close together, we are limited in our ability to determine accurately the distance to an object farther than fifty feet away. A way to determine parallax effectively at greater distances would be to establish a greater distance between the lenses of the two eyes. Such an approach is customarily used in military range finders where two more or less horizontally oriented periscopes are used for this purpose. The larger the so called base distance between the effective viewing points of the two periscope lenses becomes, the larger will be the parallactic angle. And as we have said before, the more nearly the parallactic angle approaches ninety degrees, the less on average will be the measurement error. However, if the ends of the periscope were placed so far apart as to view the object from such different perspectives that the relationship would be unrecognizable in the two films, then it would be impossible to range the object appropriately.

This description of military range finding constitutes a rough analogy to the roentgenographic stereometric case. If the two x-ray machines are placed too close together, the effect will be similar to that of a human being viewing an object at a distance greater than fifty feet and it will be impossible to obtain an appropriate stereo solution. On the other hand, if the separation between the viewing points is too great, then it will become impossible to carry out successfully the cognitive process of associating the physical features of a landmark viewed from the two perspectives. The greater simplicity of identifying anatomical structures using the stereoscopic method of Baumrind *et al* compared to biplanar images using the Broadbent method may be seen in Figure 5.

But notwithstanding the fact that it is easier to associate a structure in the paired *lateralis* films or the paired *frontalis* films shown in Figure 5 than in the *norma lateralis* and the *norma frontalis* films, the task is still difficult. The offset projections shown in Fig. 5 are frankly unfamiliar to the viewer and it is highly likely that considerable training will be required before the two images of the same point can be identified uniquely on the two films. In an attempt to solve this problem, we are conducting this study, with the purpose of developing a system to assist in training biologically oriented workers in locating the same anatomical landmarks on both films of any given x-ray stereopair. We also propose to produce

photographic stereopairs which will illustrate clearly the precise location of each metallic marker which has been imaged in the x-ray stereopairs.

Materials and Methods:

In this study, we have investigated the properties of the images of thirty-one landmarks which are conventionally used in orthodontics and craniofacial research. For each of these landmarks, separate x-ray stereo pairs in the lateral, frontal and forty-five degree left projections have been generated for each of four representative skulls. In order to facilitate quantification, a set of five metallic reference markers was placed in the upper skull and a similar set of of four markers was placed in the mandible. Stereo pairs for each of the three projections were generated for each skull with the landmarks unidentified. Following this procedure, metal spheres were placed at the location of each landmark and the skulls were re-x-rayed. However, in order to prevent the confusion which would have accompanied the placement of thirty-one metal markers simultaneously, the landmark identification process was conducted using several series of films for each skull. In each series, only a subset of landmarks was identified with metal markers. In all, four series the pairs of head films were taken for each skull. Each series included a lateral, a frontal and a forty-five degree left oblique stereo pair. In Series 1, only the nine reference markers (termed "tie points") were placed. The five tie points on the maxillofacial portion of the skull were placed on the right and left posterior regions of the supercilliary arches, the nasal tip and the right and left zygoma (Fig. 6). The four tie points on the

mandible were placed on the right and left posterior regions of the body of the mandible and the right and left anterior regions of the body of the mandible. Series 2 contained the tie points plus seven landmarks. The landmarks in this series were ANS, PNS, right and left PTM, right and left Gonion and Menton. In Series 3, in addition to the nine tie points, twelve landmarks were represented. These landmarks were Sella, Nasion, Point A, right and left Orbitale, right and left Porion, right and left Condyle, Point B, Pogonion and Basion. In Series 4, in addition to the nine tie points, twelve landmarks were represented. These consisted of stainless steel wires pointing to the mesio-buccal cusps and the mesial apices of all four first molars and to the incisal edges and apices of the upper and lower right central incisors.

The definitions employed for the landmarks were as follows:

1. Porion: The superiormost point of the external auditory meatus.

2. Sella: The midpoint of pituitary fossa as determined by inspection.

3. Nasion: The most antero-inferior point on the frontal bone at the nasofrontal suture.

4. Orbitale: The inferiormost point of the orbital margin.

5. Point A: The deepest point on the curvature of the surface of the maxillary bone between "ANS" and the alveolar crest of the upper central incisor.

6. Point B: The deepest point on the curvature of the anterior border of the mandible between pogonion and the alveolar crest of the lower central incisor.

7. Pogonion: The anteriormost point on the bony chin at the midline.

8. Menton: The inferiormost point of the mandible at the symphysis.

9. Gonion: The lowest point on the curvature of the angle of the mandible where the body of the mandible meets the ramus.

10. Condylion: The most posterior superior point on the condyle of the mandible.

11. ANS: The anteriormost point on the surface of the lower contour of anatomical anterior nasal spine at which the vertical thickness of the structure is three millimeters. (After Harvold.)

12. PNS: The most posterior extension of the palatine bone in the midline of the hard palate.

13. Basion: The most anterior point of the foramen magnum, or the juncture of the superior and inferior

surfaces of the petrous portion of the occipital bone.

14. Pterygomaxillary Fissure (PTM): An oval shaped radiolucency resulting from the fissure between the anterior margin pterygoid process of the sphenoid bone and the profile outline of the posterior surface of the maxilla. The landmark itself is at the most anterior inferior confluences of the curvatures.

15. Upper Molar Apex: The point of intersection between the long axis of the mesial root of the more anteriorly positioned upper first molar and the contour of curvature of that tooth's root surface.

16. Upper Molar Cusp: The occlusal most point of the mesio-buccal cusp of the more anteriorly positioned upper first molar.

17. Lower Molar Cusp: The occlusal most point of the mesio-buccal cusp of the more mesially positioned lower first molar.

18. Lower Molar Apex: The point of intersection between the long axis of the mesial root and the more anteriorly positioned lower first molar and the contour of curvature of that root's surface.

19. Upper Incisor Apex: The point of intersection between the long axis of the more anteriorly positioned upper central incisor and the contour of the tooth's

root end curvature.

20. Upper Incisor Edge: The tip of the incisal edge of the more anteriorly placed upper central incisor.

21. Lower Incisor Apex: The point of intersection between the long axis of the most anteriorly positioned lower incisor and the contour of the tooth's root end curvature.

22. Lower Incisor Edge: The tip of the incisal edge of the more anteriorly placed lower central incisor.

However, notwithstanding our attempt to produce rigorous operational verbal definitions, it was recognized that ambiguities might exist in the interpretation of the verbal definitions and physical errors might occur in the actual placement of the metal spheres. In order to minimize misunderstanding with these definitional problems, stereo photographs were generated for each landmark for each skull.

The procedure for attaching the markers in Series 2-4 consisted of gluing the spheres and wires to the surface of the skull with a commercially available cyanoacrylate cement (Krazy Glue). Upon the completion of the second series, the m rkers identifying the anatomical landmarks were removed before the placement of the markers for the third series. A similar procedure occured between the third and fourth series. Because it was required that the tie points placed for the first series act as reference points within the

skull for all of the subsequent series, it was important that special measures be taken to prevent them from being lost in handling. In order to fasten these spheres more securely, a small depression was drilled at the site using a high speed handpiece equipped with a round burr. The spheres were then glued into the depressions. No tie points were lost during the course of the study.

The location of Sella in the third series represented a special problem since this landmark is not located on the surface of the skull. In order to suspend the metal sphere in the middle of sella tursica, a platform of radiolucent wax was constructed within the fossa and the sphere was located upon it. By means of trial x-rays, we obtained the best position of Sella which was confirmed with stereo photographs.

As mentioned previously, lateral, frontal and forty-five degree left stereo pairs were taken within each series for each skull. All x-ray films were taken with the skull positioned such that Frankfort Plane was horizontal. This orientation was checked using a carpenter's level (See Fig. 7). Just as it was important to insure that the nine tie points not move between series, it was also important that the skulls be returned to the same position in the cephalostat for successive series of films. In order to guarantee this condition, a surveying theodolite was employed (See Fig. 8). This instrument was borrowed from the Civil

Engineering Department, University of California, Berkeley and it was used under the supervision of Sean Curry and Bernd Wand. Stereo x-ray films were exposed using the dedicated clinical stereo apparatus of the University of California, San Francisco, School of Dentistry (See Fig. 3). This apparatus was described in references 12 and 13. The stereo photographs were taken using a fully calibrated stereo camera with a nodal point subject distance of twenty-one inches. This apparatus is shown in Fig. 9 and has also been reported (15,16). All exposures were made for one second at f/22 using Plus-X Pan film. The format size for this camera is approximately seventy-five by one hundred millimeters. All films were processed to produce stereo pairs viewable using any hand-held stereoscope with an image separation of fifty-seven millimeters. (Simple hand-held stereoscopes satisfying these criteria are available from American Optical Company.)

After all x-rays and photographs had been made, the stereo x-ray images for all the lateral series and the frontal and forty-five degree series for Skull 1 were digitized using the standard hardware and software protocols of the University of California, San Francisco, Craniofacial Research Instrumentation Laboratory (12,17). Following the digitization of the individual x-ray film, the STEREO program from this program package was used to obtain three dimensional coordinates for each metal marker from each series. Then, using the MERGE program from this program

set, data from all four series for each skull were merged into a common map whose frame of reference was determined by the metallic markers at Sella, Nasion and Point A of the third series. (Appendix 2).

Digitization and computation of these stereo films involved the following set of operations:

First, each x-ray image was digitized (By the program module DIGIT) to obtain the two dimensional coordinates of all metal markers imaged upon it. This operation, was repeated until a reliability of 0.015 mm had been achieved for all metal markers. The average of the two satisfactory digitizations (generated by the program module, AVPIC) was then utilized in the next step.

Second, the program STEREO used the average digitization values from the two films of each stereo pair to produce a single unified three dimensional coordinate map.

Third, the three dimensional coordinate maps from Series 2, 3 and 4 for each skull were merged on the known locations of the tie point markers common to them (program module, MERGE). Since the mandible is not anchored unequivocally to the calvarium, it is not possible to be sure that the two structures bore the same relationship to each other in all series, even for the same skull. For this reason, two separate acts of merging were performed. The metal markers representing the anatomical structures in the

calvarium and the maxillary portions of the skull were merged on the upper facial implant markers while the anatomical markers representing landmarks in the mandible were independently and separately merged upon the mandibular implant markers. The purpose of this merging operation was to produce a three dimensional coordinate map representing the coordinate locations of all metal markers on the skull as if the several series had been superimposed in a kind of a mathematical "triple exposure".

The final mathematical procedure in the project involved a series of four steps. These were performed separately for each projection (lateral, frontal and 45 degrees left) on each skull.

Step 1. The locations of the tie points on the Series 1 three dimensional coordinate map were re-expressed in terms of a frame of reference determined by an average of the four fiducial points. This resulted in a set of output values in which the x y plane was identical with the film datum plane (within limits of the method error).

Step 2. In this step all the coordinate values of the tie points and anatomical marker spheres from the merged maps from Series 2, 3 and 4 were remerged onto the re-expressed Series 1 points. Here again, the upper and lower groups of anatomical markers spheres were merged separately based on their respective sets of tie points. At this point, the remerged Series 2, 3 and 4 marker spheres had the

same coordinates (except for measurement error) as if the sphere had actually been present on the Series 1 stereo films.

Step 3. In this third step, the coordinates of all the markers which had been remerged onto the Series 1 tie points as well as the tie points themselves were changed to a frame of reference in which the origin was again located at the Sella marker, the x axis passed through the Nasion marker and the x y plane passed through the Point A marker.

Step 4. In this final step of the procedure, the three dimensional coordinate map constructed in Step 2 above was decomposed to form the two members of a stereo pair by means of a mathematical operation which is conceptually the inverse of the construction of a three dimensional coordinate map from information on two two dimensional maps, one for the centered film and one for the offset film of the combined lateral stereo pair in the Series 1 datum. Using a Tektronix's 4662 xy Plotter, we then generated separate full scale graphic transparent overlays for centered and offset films for each lateral stereo pair. Full size, 1:1 transparencies for the lateral skull x-ray stereo films for Skulls 1 through 4, together with matching 1:1 scaled overlays, as well as complete sets of stereophotographs of the landmarks identified on Skulls 1-4 will be all assembled in the future into a comprehensive training atlas.

Results

The combined stereophotographic and stereo roentgenographic method used in this study provided a set of head films with associated overlays suitable for use in improving the training of craniofacial biologists in the identification of common craniofacial landmarks on lateral skull head films. It has also provided a set of stereo photographs as a qualitative means for landmark identification in three dimensions. Fach landmark was located quantitatively on each of the pairs of all lateral skull stereo x-rays with a point location reliability of 0.015 mm. The location of each landmark was expresed in a two dimensional coordinate system for each separate pair of a stereo film (*norma lateralis and norma frontalis*), and also expressed in a three dimensional coordinate system for each pair of stereo x-ray films.

The photographic and numerical materials which constitute the result of the operations described in the Methods section are included in the Appendix to this paper. Part 1 of this Appendix contains representative reduced photographic prints of the lateral, frontal, and forty-five degree left oblique stereo x-rays for Skull 1 as well as stereo photographs for a number of the landmarks identified on that skull. (Complete sets of such photographs have been produced for all four skulls and will later be assembled

into a comprehensive training atlas.)

The stereo photographs of the landmarks (but not the pictures of the x-rays themselves) may be viewed three dimensionally using the small hand stereoscope which has been supplied. In order to observe these images stereoscopically, lay the Appendix flat upon a well illuminated surface and hold the stereoscope against the eyes with its handle in your right hand. The plane of the stereoscope should be aligned parallel to the plane of the Appendix and about six inches above its surface. The imaginary line joining the centers of the eyes (termed the base line) should be parallel to the lines forming the upper and lower borders of the illustrations. Move the head slowly toward and then away from the printed page while looking at the illustration until the middle one of the three images you see starts to become three dimensional. If your eyes are reasonably well balanced, you should begin to see a three dimensional "stereoscopic" image after a few moments of accommodation. As you continue to look at the image it should get sharper and sharper. Sometimes it takes a few minutes to "lock onto" the first image, but after you see the first one, the others should become progressively easier.

Part 2 of the Appendix contains examples of computer output representing the techniques by means of which the graphic values of the implant markers shown in Part 1 were reduced to digital form.

The matching overlays generated for the lateral stereo films of Skull 1-4 indicate the location on the centered and offset films of the stereo pair at which the anatomical marker spheres (which had been placed in position on the films of Series 2, 3 and 4) would have been imaged if the metal makers had actually been situated on the Series 1 film. These lateral stereo pairs are meant for use in training subsequent workers in precision landmark location in three dimensions.

Discussion:

The graphic output of this study is likely to be of assistance to craniofacial investigators in improving the reliability and validity with which commonly used cephalometric landmarks are located on x-ray stereopairs and possibly on conventional individual "centered" cephalograms as well. The numerical data should also assist in the empirical determination of the limitations in accuracy of locating unambiguous markers using the precise geometry of the Baumrind stereo cephalometric system. It is contemplated that in a subsequent expansion of this project, overlays similar to those here developed for the lateral stereopairs will also be developed for the frontal and forty five degree oblique stereopairs and that additional sets of landmarks of interest may also be studied.

In the course of conducting this project, a number of interesting technical problems were faced and solved. The use of the theodolite (surveying device) as a mechanism for producing reliable replacements of the skulls within the cephalostat was very successful notwithstanding the presence of some residual errors. For the stereo photographs, there were problems in developing an optimal lighting system. In solving this problem, important assistance was provided by Mr. Douglas Symes, technical photographer and consultant to the Craniofacial Research Instrumentation Laboratory. Mr. Symes was also responsible for the processing of all film

and the printing of all stereopairs, operating under the supervision of the author and Dr. Baumrind.

Even though opaque markers were used, some landmarks were consistently more difficult to locate than others. Particularly inconsistent was the location of Orbitale. When viewed from the lateral perspective this landmark differs markedly in sagittal position from case to case. Additionally, the identification on the norma frontalis head film of most of the ordinary landmarks in the midsagittal plane (Sella, Nasion, ANS, Point A) proved to be considerably more difficult than had been anticipated. The existence of this problem adds to the difficulty in obtaining valid three dimensional landmark location using Broadbent type orthogonal film pairs.

Notwithstanding careful exposure, some of the metal markers located at the osseous points, Porion, Gonion and Condylion, were poorly visualized. Attempts to vary our exposure technique so as to give greater penetration in this area tended to result in overexposure and burn-out in thinner regions of the facial bones. Similar difficulties were encountered in Series 4 with some of the stainless steel markers which were used to demonstrate root structures.

The inconsistency in the location of Orbitale from the lateral perspective and the difficulties in locating landmarks as Sella, Nasion, ANS and Point A on norma frontalis

head films makes it more unlikely that these landmarks can be reliably located in three dimensions on orthogonally positioned film pairs. The identification of conjugate pairs of points on the coplanar stereo x-ray films seems certainly more promising for the midsagittal landmarks, for the gonial angles and for a number of other frequently located anatomical reference points. However, in the area of the teeth themselves, the problem of overlapping structures appears to be sufficiently great so that reliable identification of conjugate images of dental landmarks on lateral stereo pairs may prove to be an unrealistically difficult task. Such a reality would tend to emphasize the importance of developing better methods of locating dental structures themselves on study casts, on images of study casts or on direct intraoral images and of merging those data into stereo head film data using techniques of the general type described earlier by Baumrind et al. (18).

In the area of the stereo x-ray films themselves, it must be recorded that consequential problems were encountered in terms of the dynamic range of the film, particularly with regard to the task of locating metal markers overlying the petrous portion of the temple bone.

Summary

The difficulties in obtaining three dimensional x-ray information on pairs of films oriented at right angles to each other have been discussed. We have investigated the use of a coplanar stereometric system in an attempt to solve the problem of accurate identification of craniofacial landmarks on stereo head films and the determination of their three dimensional locations in space. A combined stereophotographic and stereo x-ray image set for training craniofacial biologists so as to improve the accuracy of identification of common craniofacial landmarks in three dimensions has been developed. The landmarks were located on each of the films of a stereo pair of lateral skull x-ray films. Because one of the films, the norma laterlis, is equivalent to a standard lateral cephalogram, the clinician can also apply these methods to standard head films. Qualitative means for identification of the landmarks precisely in the positions in which they were x-rayed are supplied in the form of the appended stereophotographs. It has also provided a quantitative measure of the reliability of three dimensional landmark locations on stereo head films. We obtained a reliability in point location of 0.015 mm for unambiguous metal targets. The exact distribution of errors in locating the anatomical landmarks themselves will be undertaken in later studies.

References

1. Herron, R.: Biostereometric measurement of body form, Yearbook of Physical Anthropology, vol. 16, pp. 80-121, 1972.

2. Choulant, L.: History and bibliography of anatomic illustration. Translated and annotated by M. Frank Hafner. Publishing Company, New York, 1962.

3. Gadol, J.: Leon Battista Alberti, Universal man of the early Renaissance, University of Chicago Press, Chicago, 1969.

4. Brewster, Sir David.: The stereoscope, its history, theory and construction. London : J. Murray, pp. 18-27, 1856.

5. Baumrind, S.,and Moffitt, F.H.: Mapping the skull in 3-D, J. Calif. Dent. Assoc. 48: 22, 1972.

6. Lasker, G.W., Tyzzer, R.N.,: Physical Anthropology, third ed. CBS College Publishing Holt, Rinehart and Winston, New York, 1982.

7. Slotkin, J.S.: Readings in early Anthropology, Aldine Publishing Co., 1965.

8. Mackenzie-Davidson, J.: Stereoscopic photographs, Brit. Med. J., pp.1697-1698, Dec. 3, 1898.

9. Broadbent, B.H.: A new x-ray technique and its application to orthodontia, Angle Orthod. 1:45, 1931 (reprinted in Angle Orthod. 51: 93, 1981).

10. Savara, B.S.: Application of photogrammetry for quantitative study of tooth and face morphology. Am. J. Phys. Anthro. vol. 23, pp. 427, 1965.

11. Rune, B., Jacobsson, S., Sarnas, K.V., Selvik, G.: A roentgen stereophotogrammetric study of implant stability and movement of segments in the maxilla of infants with cleft lip and palate. Cleft Pal. J., vol. 16:3 pp. 267-278, July 1979.

12. Baumrind, S., Moffitt, F., Curry, S., and Isaacson, R.J.: A dedicated stereo-photogrammetric x-ray system for craniofacial research and treatment planning, Proceedings of the Society of Photo-Optical Instrumentation Engineers, vol. 361 (39): 200-209, 1982.

13. Baumrind, S., Moffitt, F., Curry, S.: Three-

dimensional x-ray stereometry from paired coplanar images: A progress report, Am. J. Orthod., vol. 84: 4, pp. 292-312, 1983.

14. Baumrind, S., Moffitt, F.H., and Curry, S.: The geometry of three-dimensional measurement from paired coplanar x-ray images. Am. J. of Orthod., vol. 84-04, pp. 313-322, 1983.

15. Curry, S., Moffitt, F.H., Symes, D., Baumrind, S.: A family of calibrated stereometric cameras for direct intra-oral use. Proceedings of the Society of Photo-Optical Instrumentation Engineers, vol. 361-02, pp. 7-14,1982.

16. Baumrind, S. Moffitt, F.H., Symes, D.: Specialized stereo cameras for use in dental research. J. Dent. Res. (Special issue) vol. 57:1153, 1978.

17. Baumrind, S., and Miller, D.M.,: Computer-aided head film analysis: The University of California San Francisco Method, Am. J. of Orthod. 78: 41-65, 1980.

18. Baumrind, S., Curry, S. : Merging of data from different records in craniofacial research and treatment. Handbook of the 1984 workshop on non-topographic photogrammetry, American Society of Photogrammetry, July 1984.

Appendix

Part 1:

Section A. Representative photographs of x-ray films of skull 1 (X-ray stereopairs 1 -6).

Section B. Representative stereophotographs of skull 1 at the time series 2, 3 and 4 were taken.

Part 2: Examples of computer output representing graphic values of the implant markers.

Part 1
Seccion A.

X-ray stereopair 1. Lateral skull films of series 1
(series 1 shows nine reference markers
and no anatomical points).
Top: centered film
Bottom: offset film

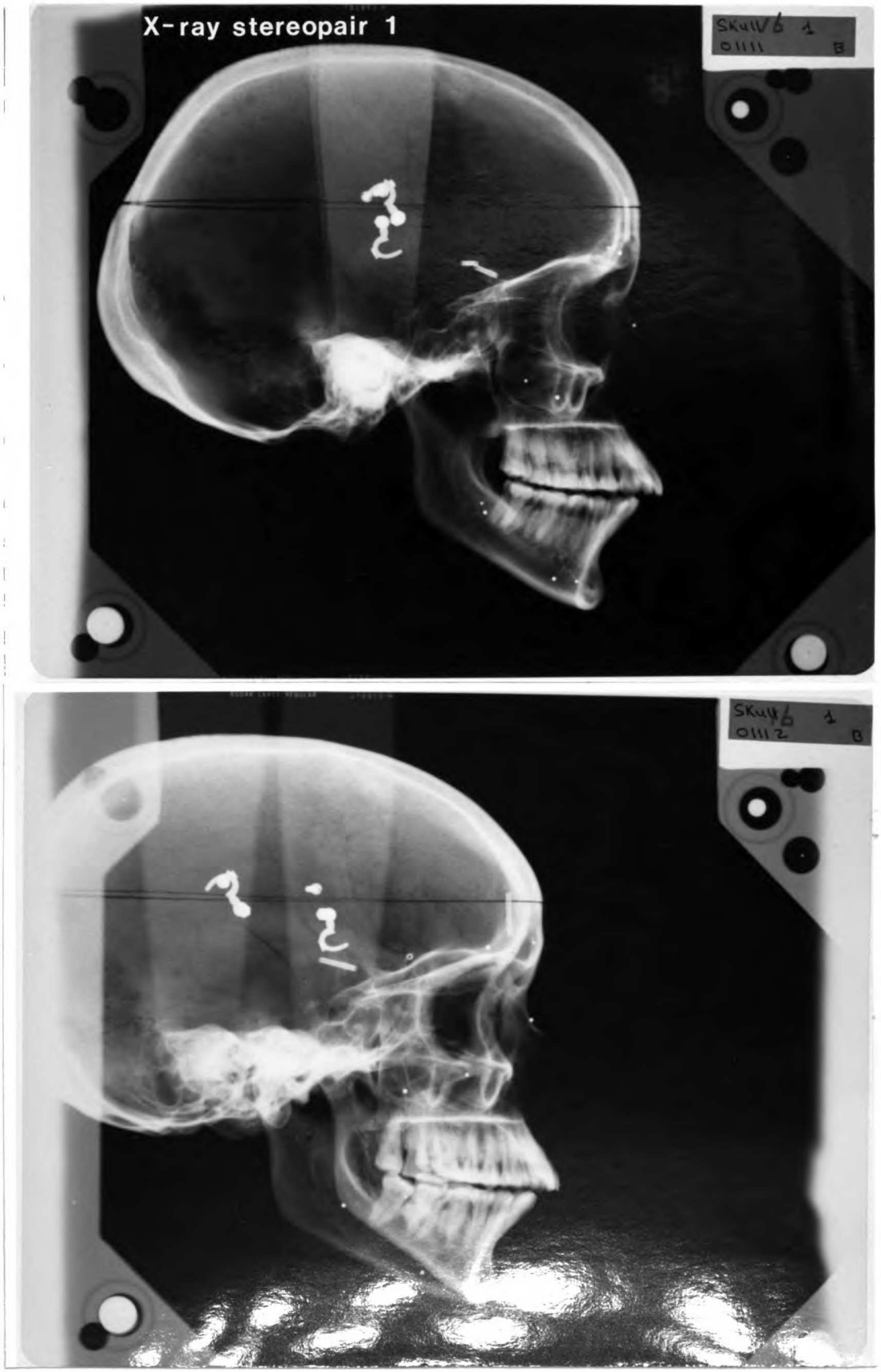
X-ray stereopair 1

X-ray stereopair 2. Lateral skull films of series 2
(series 2 shows nine reference markers
plus metal markers at ANS, PNS, PTM -R and L-,
gonion -R and L- and menton. Bigger size
spheres differentiates the right side of
bilateral structures from the left side).
Top: centered
Bottom: offset

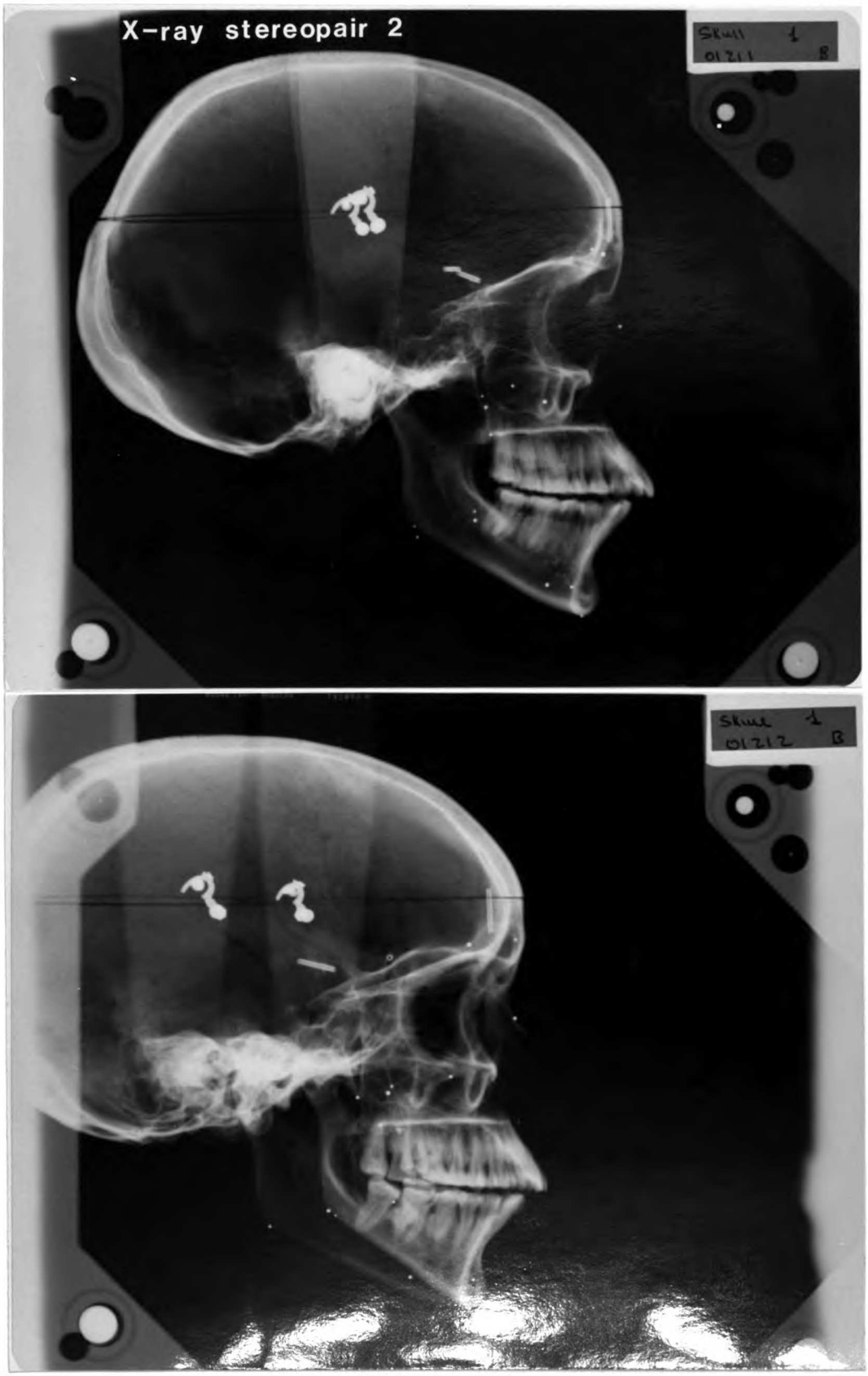
X-ray stereopair 2
Skull 1
01211 B
Skull 1
01212 B

X-ray stereopair 3. Lateral skull films of series 3 (series 3 shows nine reference markers plus metal markers at sella, nasion, Point A, orbitale (R & L), porion (R & L), Condylion (R & L), Point A, pogonion and basion.
Top: centered film
Bottom: offset film

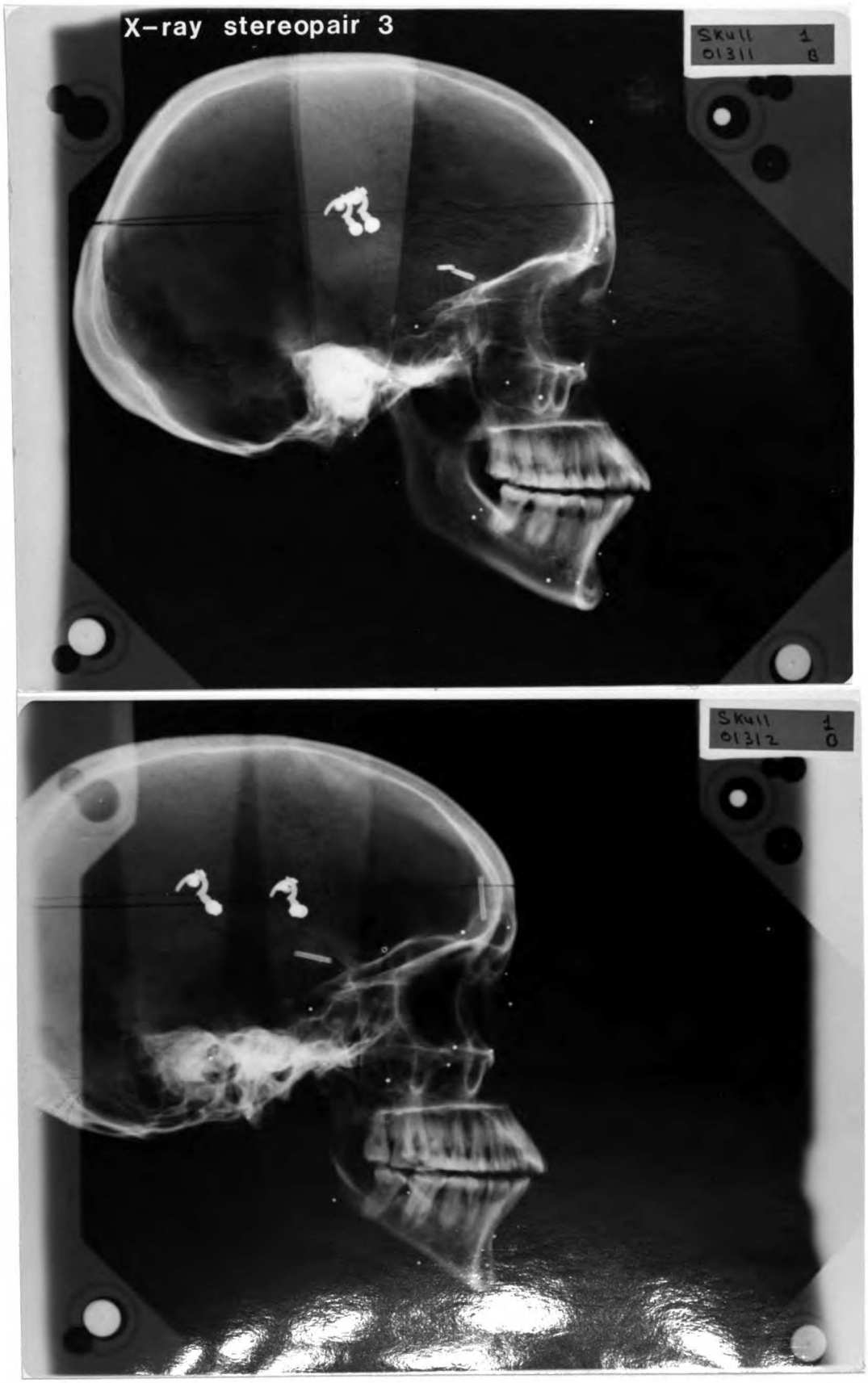
X-ray stereopair 3
SKULL 1
01311 B
SKULL 1
01312 B

X-ray stereopair 4. Lateral skull films of series 4 (series 4 shows nine reference markers plus steel wires indicating the mesio-buccal cusps and mesial roots of all four first molars, and the incisal edges and apices of upper and lower right central incisors.
Top: centered film
Bottom: offset film

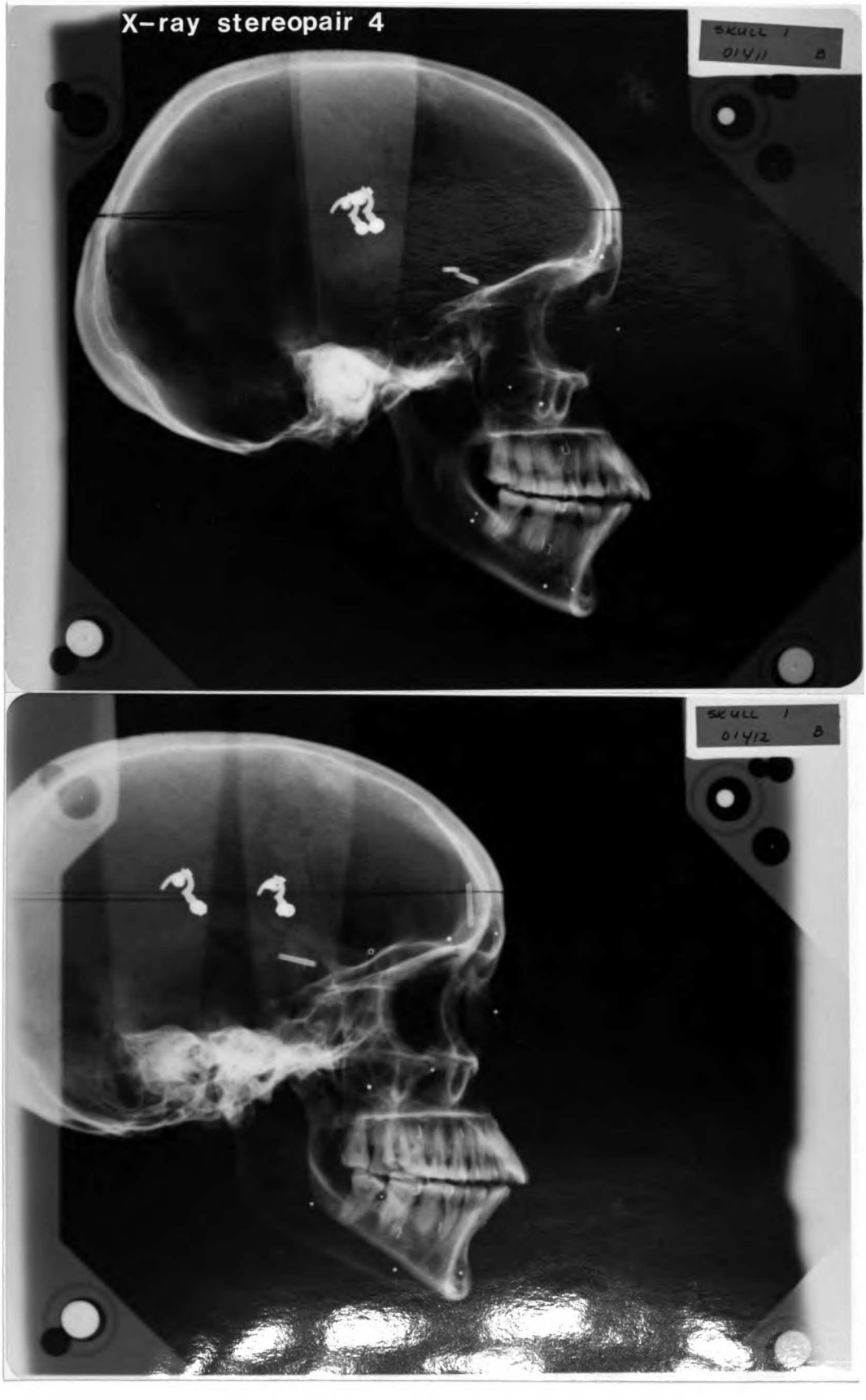
X-ray stereopair 4
SKULL 1
01411 B
SKULL 1
01412 B

X-ray stereopair 5. 45 degree left skull films of series 2.
Top: centered film
Bottom: offset film

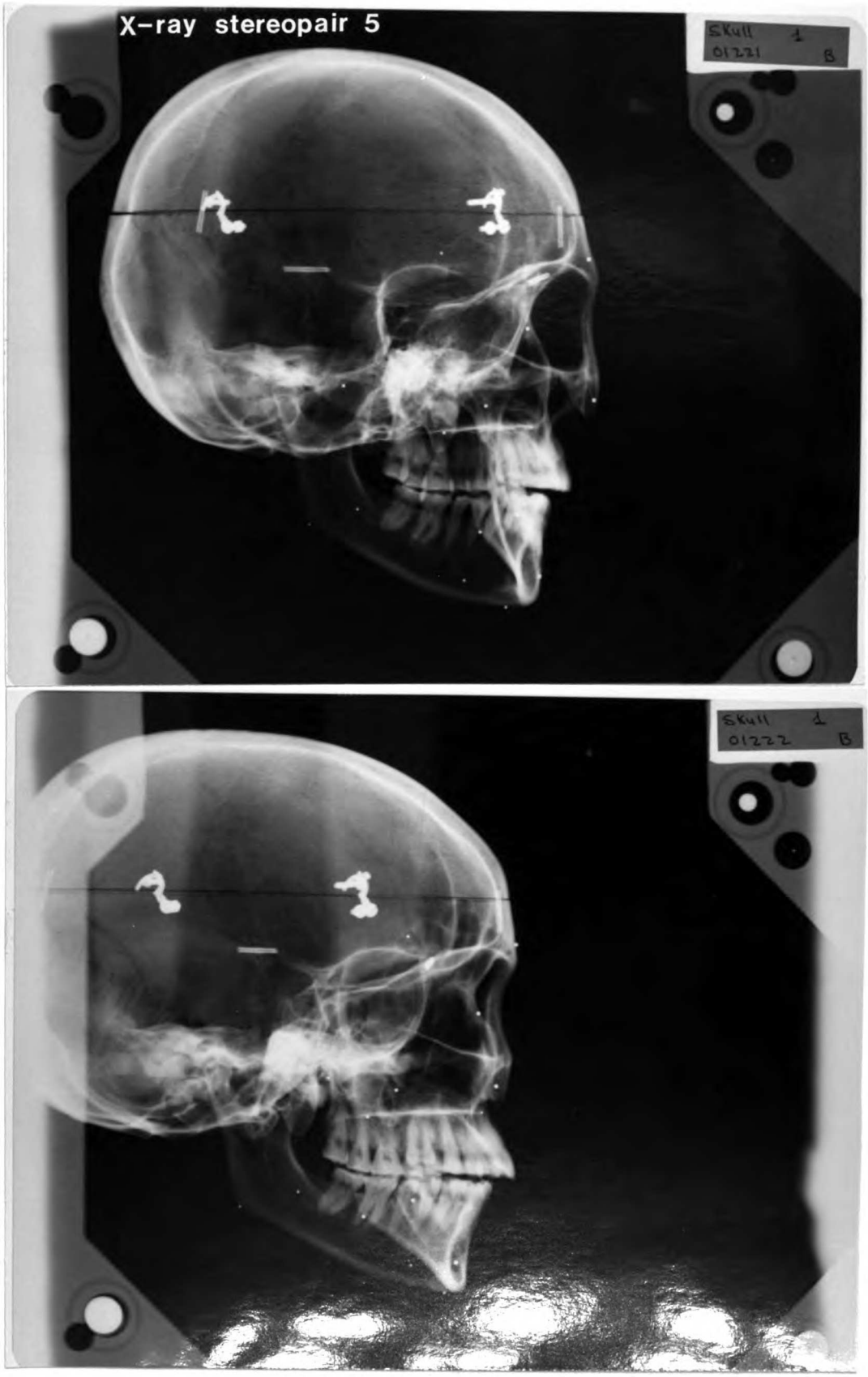
X-ray stereopair 5
SKULL 1
01221 B
SKULL 1
01222 B

X-ray stereopair 6. Postero-anterior (PA) skull films of series 2.
Top: centered film
Bottom: offset film

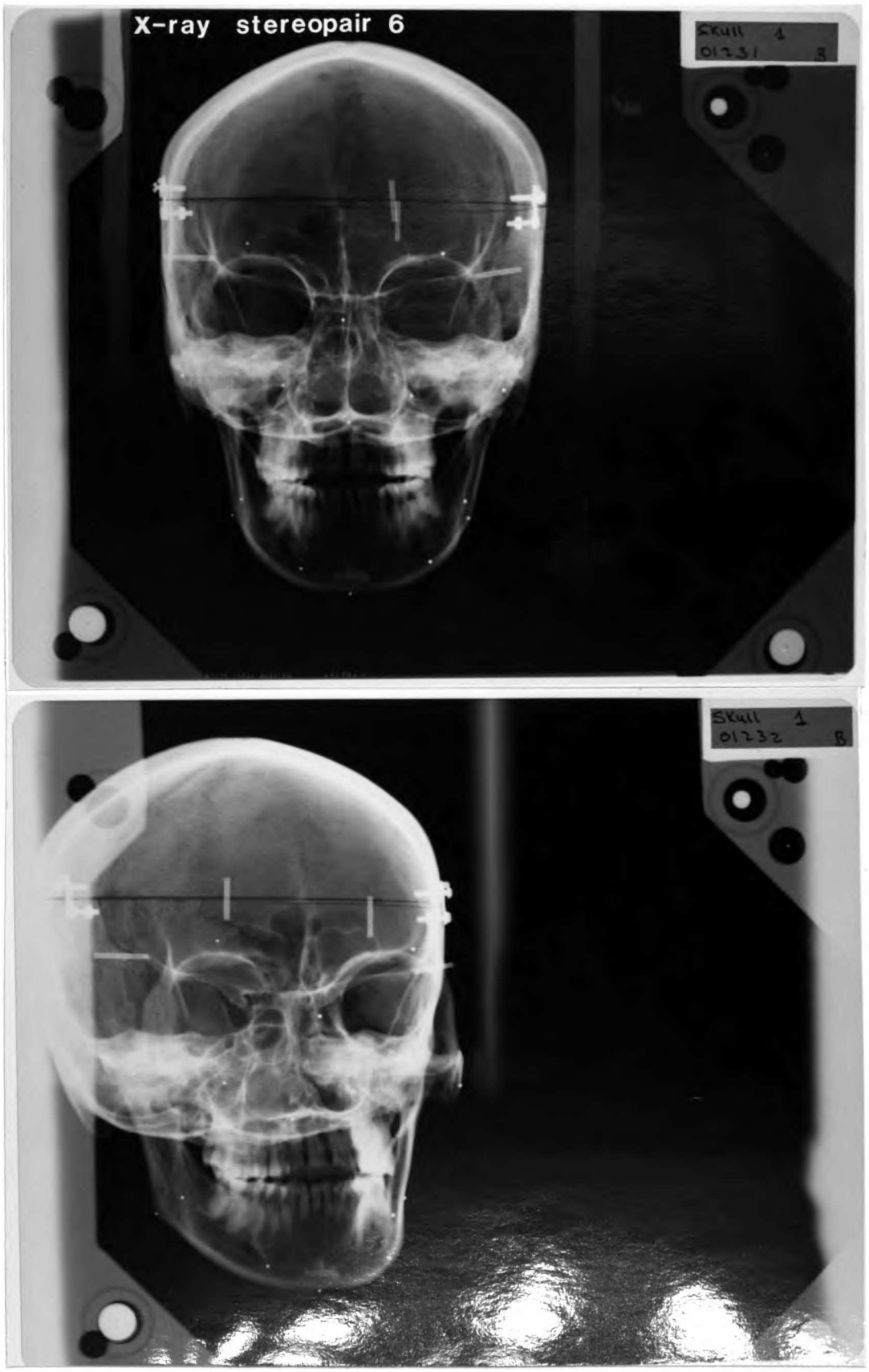
X-ray stereopair 6
SKULL 1
01231 R
SKULL 1
01232 R

Top. Series 2, frontal view showing ANS

Bottom. Series 2, view of mandible showing menton and gonion (R & L).


1
1
SKULL
1.2.1

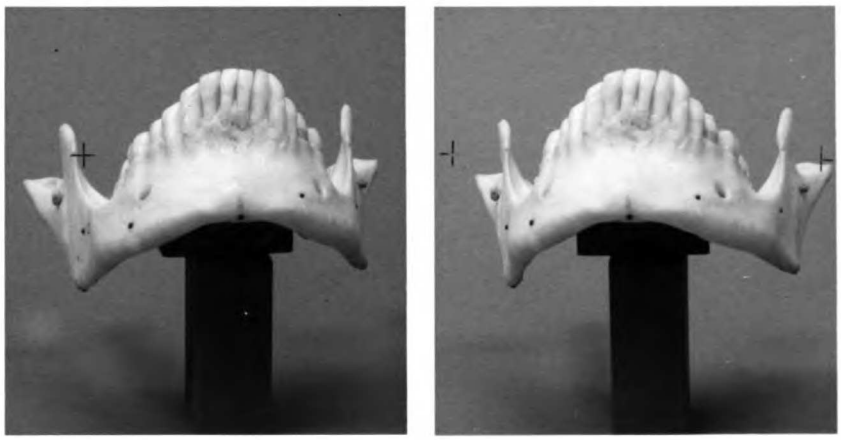

Top. Series 2 left lateral view showing ANS and PTM (left).

Bottom. Series 2, tilted palatal view showing (enlarged) PTM (left) and PNS.

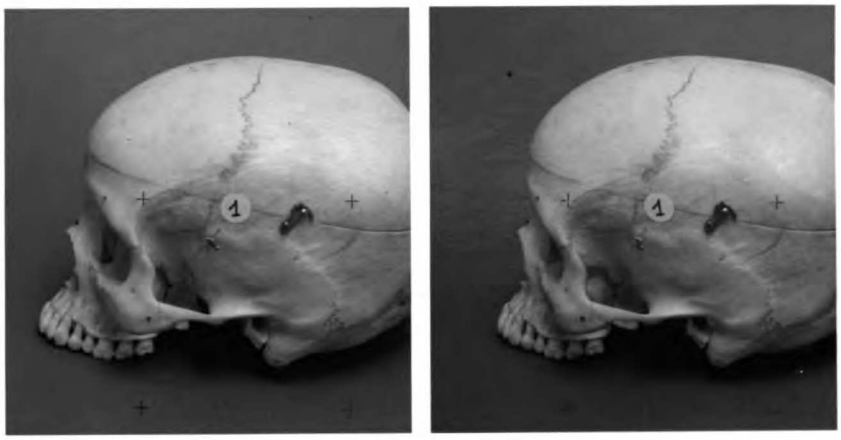
1
1

Top. Series 2, lateral view showing PTM (right) and ANS.

Bottom. Series2, lateral view (enlarged) showing PTM (right) and ANS.


1
1

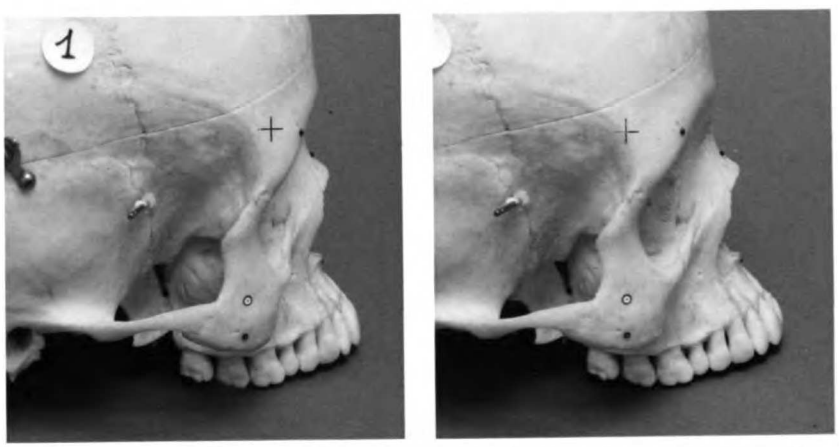
1

Top. Series 2, palatal view showing PNS.

Bottom. Series 2, palatal view (enlarged) showing PNS.

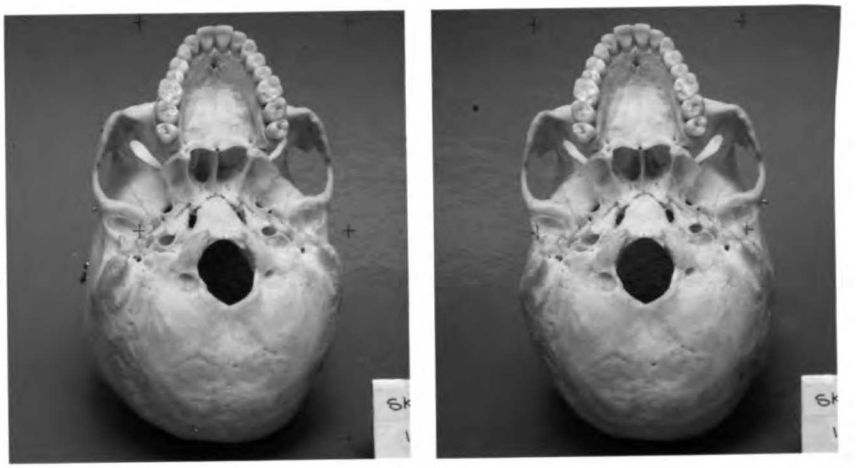

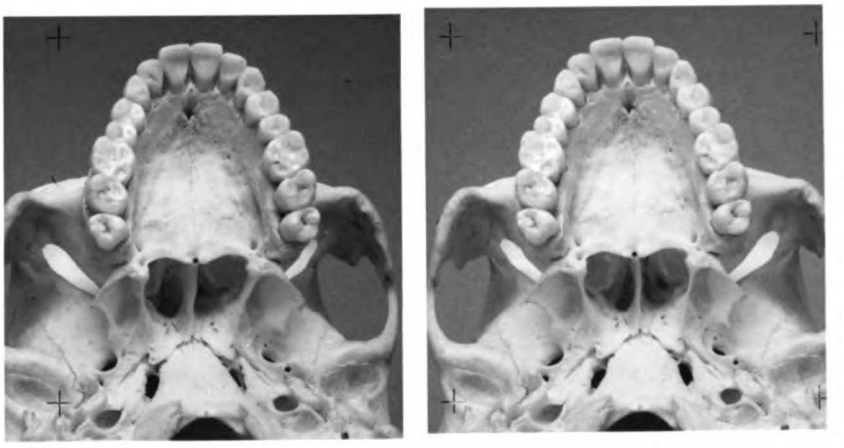

Top. Series 2, inferior view of mandible showing gonion (R & L) and menton.

Bottom: Series 2, oblique view of mandible showing gonion (R & L) and menton.

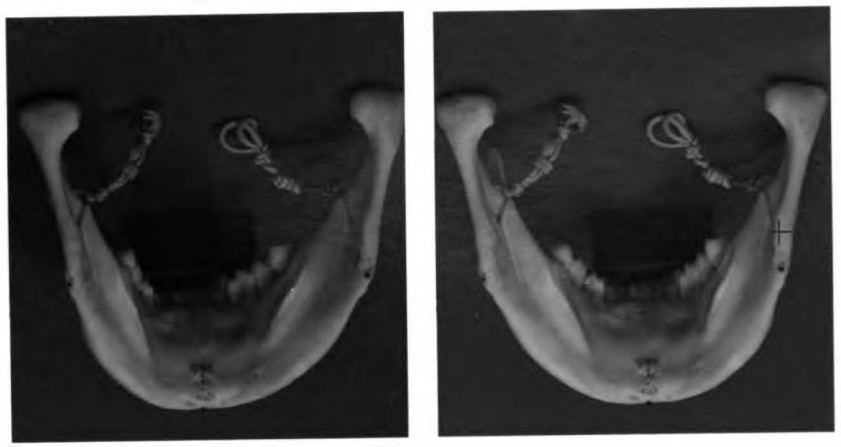

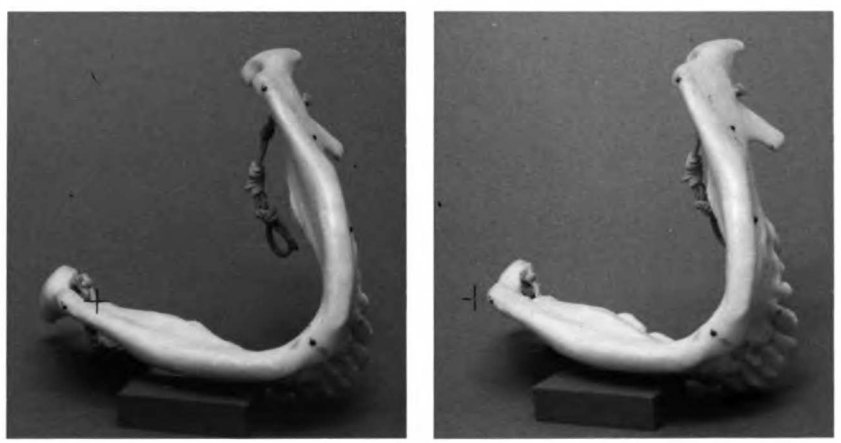

Top. Series 3, frontal view showing nasion, orbitale (R & L), Point A, Point B and pogonion.

Bottom. Series 3, frontal view (enlarged) showing orbitale (R & L) Point A, Point B, and pogonion.


1
1

Top. Series 3, internal view of cranial base showing marker identifying sella.

Bottom. Series 3, bottom view of the cranium showing basion.

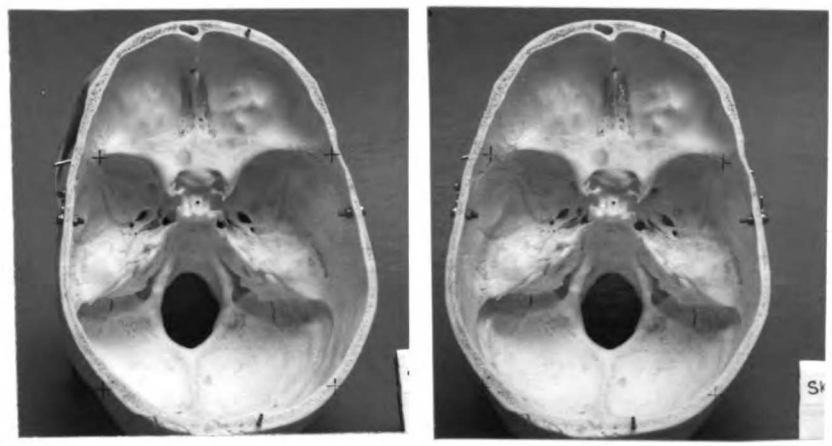

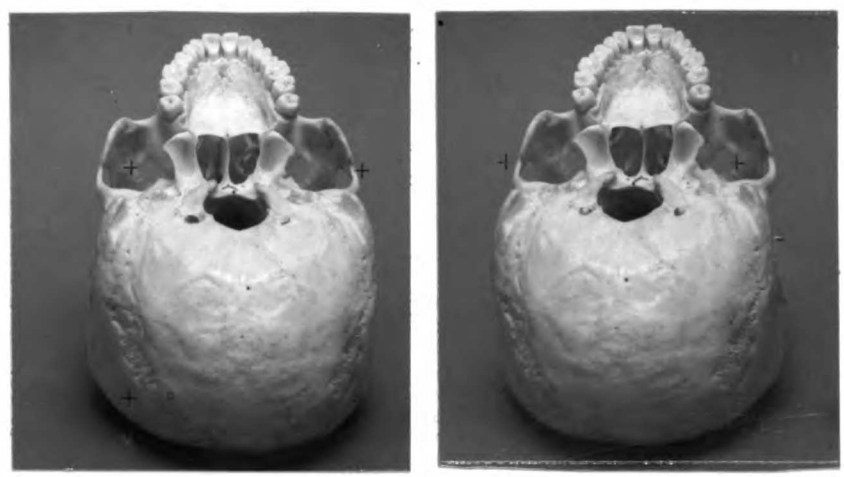

Top. Series 3, lateral view showing nasion, orbitale (R), Point A, porion (R), Point B and pogonion.

Bottom. Series 3, lateral view (enlarged) showing nasion, orbitale (R), Point A, Point B and pogonion.

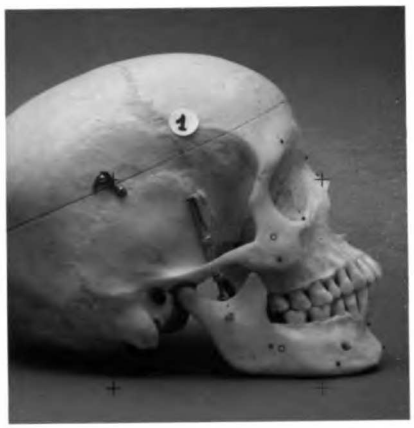
1


1

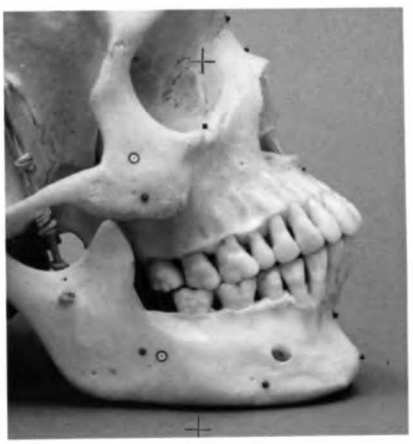

Top. Series 3, lateral view (tilted) showing nasion, orbitale (R), porion (R) and Point A.

Bottom. Series 3, lateral view (tilted) showing nasion, porion (L) and basion.

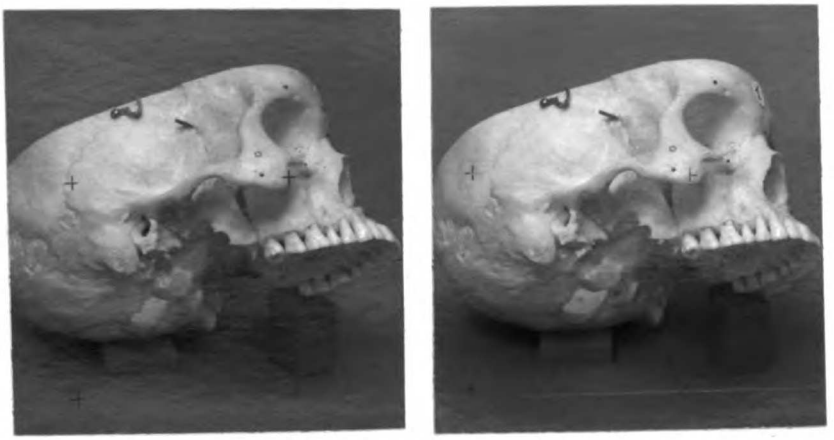

Top. Series 3, posterio view of mandible showing condylion (R & L).

Middle. Series 3, lateral view of mandible (left) showing condylion (R & L), Point B and pogonion.

Bottom. Series 3, lateral view of mandible (right) showing the same as above (middle).

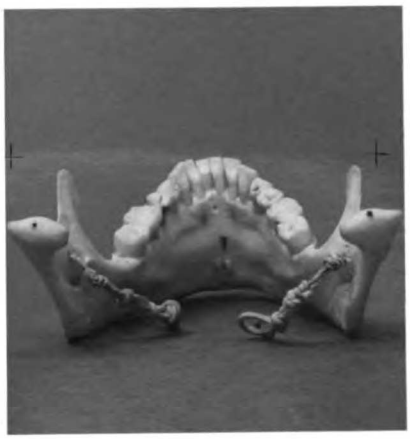

Top. Series 4, frontal view showing metal tooth markers (L shaped on the right and straight wires on the left) designating right central incisors edge and apix, mesio-buccal cusps and mesial apices of all four first molars.

Bottom. Series 4, frontal view (enlarged) showing same as Top.

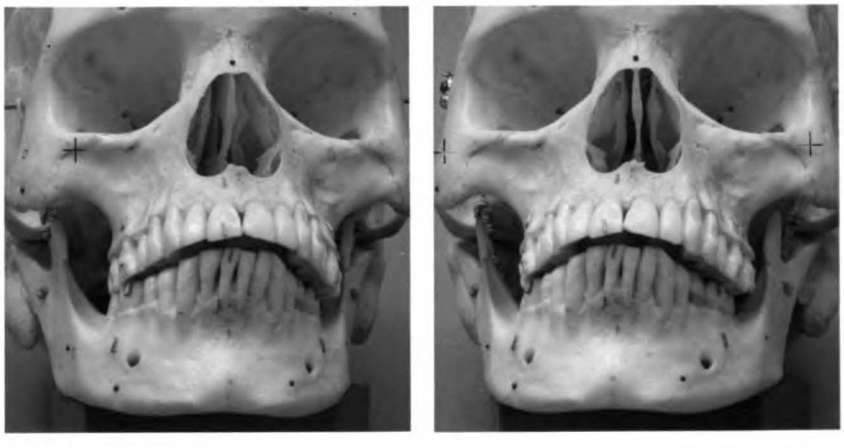

Top. Series 4, lateral view (tilted) showing metal tooth markers pointing at the upper right central incisor edge and apix, and at the upper right first molar mesio buccal cusp and mesial root.

Bottom. Series 4, view of mandible showing metal tooth markers at lower right incisor edge and apix, and lower first molars mesio-buccal cusps and mesial roots.

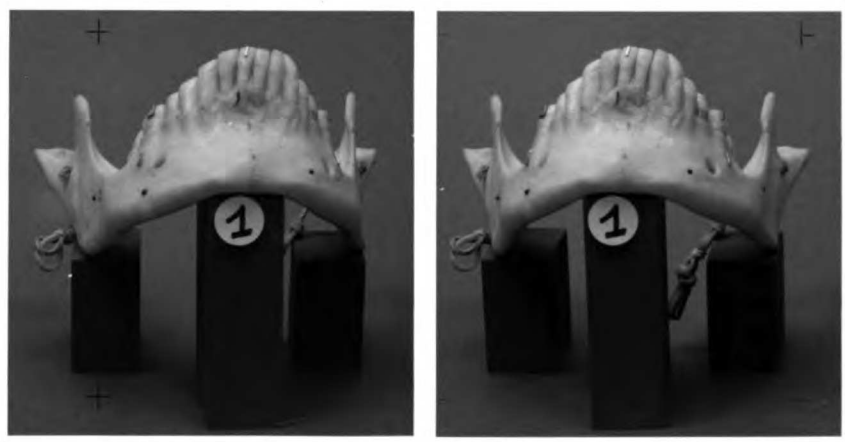
1
1

Top. Series 4, right lateral view of mandible showing metal tooth markers designating the mesio-buccal cusp and mesial root of lower right first molar.

Bottom. Series 4, left lateral view of mandible showing metal markers designating the mesio-buccal cusp and mesial root of lower left first molar.

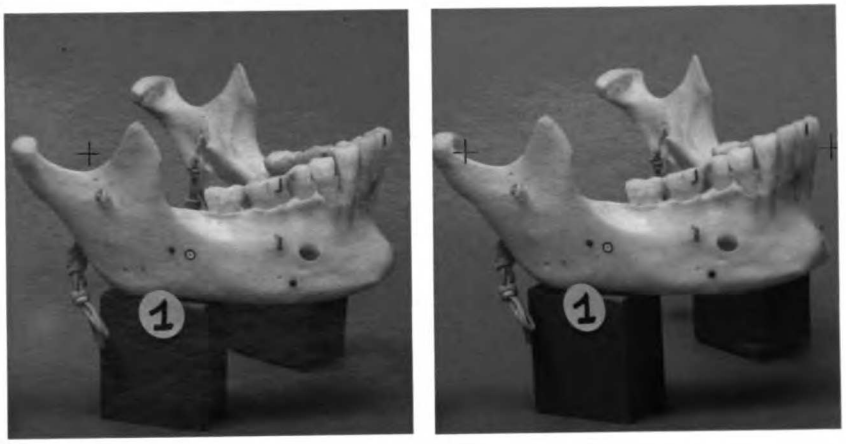
1
1


1
1

Part 2.

CENTERED TRACING FILE

```
H                DATE FILE CREATED = 29. 2.  84
8402CENTERED 1111     ATLAS
 11
                                    X       Y
  0 A  :A FIDUCIA 821    64.70  107.20
  0 B  :B FIDUCIA 822    61.70  287.60
  0 C  :C FIDUCIA 823   285.50  289.30
  0 D  :D FIDUCIA 824   308.80   96.40
  0  1:R SUPRCIL1201    241.50  238.70
  0  2:L SUPRCIL1202    237.50  240.60
  0  3:NASAL TP 1203    246.80  213.30
  0  4:R ZYG TP 1204    220.10  187.80
  0  5:L ZYG TP 1205    208.90  193.60
  0  6:R POSTMAN1206    195.40  147.50
  0  7:L POSTMAN1207    196.70  149.90
  0  8:R ANTMAN 1208    220.80  124.30
  0  9:L ANTMAN 1209    230.10  123.00
  0 10:ANS         20    999.99  999.99
-----------------------------------------
  0 40:LL 6 APEX1230    999.99  999.99
 -7
H                DATE FILE CREATED = 29. 2.  84
8402CENTERED 1111     ATLAS
 98
  0 A  :A FIDUCIA 821    64.80  107.20
  0 B  :B FIDUCIA 822    61.60  287.50
  0 C  :C FIDUCIA 823   285.60  289.20
  0 D  :D FIDUCIA 824   308.70   96.40
  0  1:R SUPRCIL1201    241.50  238.70
  0  2:L SUPRCIL1202    237.50  240.50
  0  3:NASAL TP 1203    246.80  213.40
  0  4:R ZYG TP 1204    220.10  187.80
  0  5:L ZYG TP 1205    209.00  193.60
  0  6:R POSTMAN1206    195.50  147.50
  0  7:L POSTMAN1207    196.70  149.90
  0  8:R ANTMAN 1208    220.90  124.30
  0  9:L ANTMAN 1209    230.10  122.90
  0 10:ANS         20    999.99  999.99
-----------------------------------------
  0 40:LL 6 APEX1230    999.99  999.99
 -7
```

Dashes represent lines omitted in this example.

Individual tracing values for two digitizations of skull 1, series 1 lateral centered film.

OFFSET TRACING FILE

```
H                DATE FILE CREATED = 29. 2.  84
84020FFSET   1112     ATLAS
 11
                                  X       Y
  0 A  :A FIDUCIA 821    72.50  107.50
  0 B  :B FIDUCIA 822    71.40  287.80
  0 C  :C FIDUCIA 823   295.00  287.40
  0 D  :D FIDUCIA 824   316.30   94.40
  0   1:R SUPRCIL1201   199.00  237.50
  0   2:L SUPRCIL1202   215.10  239.20
  0   3:NASAL TP 1203   214.40  212.00
  0   4:R ZYG TP 1204   170.20  186.80
  0   5:L ZYG TP 1205   191.90  192.60
  0   6:R POSTMAN1206   149.30  146.60
  0   7:L POSTMAN1207   173.10  148.80
  0   8:R ANTMAN 1208   177.50  123.10
  0   9:L ANTMAN 1209   200.20  121.80
  0 10:ANS         20   999.99  999.99
-------------------------------------
  0 40:LL 6 APEX1230   999.99  999.99
 -7
H                DATE FILE CREATED = 29. 2.  84
84020FFSET   1112     ATLAS
 98
  0 A  :A FIDUCIA 821    72.40  107.60
  0 B  :B FIDUCIA 822    71.10  287.80
  0 C  :C FIDUCIA 823   294.90  287.60
  0 D  :D FIDUCIA 824   316.30   94.40
  0   1:R SUPRCIL1201   199.00  237.50
  0   2:L SUPRCIL1202   215.10  239.20
  0   3:NASAL TP 1203   214.40  212.00
  0   4:R ZYG TP 1204   170.20  186.80
  0   5:L ZYG TP 1205   191.90  192.60
  0   6:R POSTMAN1206   149.30  146.70
  0   7:L POSTMAN1207   173.10  148.80
  0   8:R ANTMAN 1208   177.50  123.20
  0   9:L ANTMAN 1209   200.20  121.70
  0 10:ANS         20   999.99  999.99
-------------------------------------
  0 40:LL 6 APEX1230   999.99  999.99
 -7
```

Dashes represent lines omitted in this example.

Individual tracing values for two digitizations of skull 1 series 1 lateral offset film.

CENTERED AVEPIC FILE

```
8402     0.99060     3  8 84
01111 R 02/15/84     /  /      S. 1, SK 1
                        X         Y
 821 A :A FIDUCIA     0.00      0.00     0.00     0.00     0.00
 822 B :B FIDUCIA   -10.97    178.34     0.01     0.00     0.00
 823 C :C FIDUCIA   210.54    189.83     0.01     0.00    -0.00
 824 D :D FIDUCIA   241.94      0.00     0.00     0.00    -0.00
1201  1:R SUPRCIL   169.16    137.88     0.00     0.00     0.00
1202  2:L SUPRCIL   165.12    139.53     0.00     0.00    -0.00
1203  3:NASAL TP    175.51    113.02     0.00     0.01     0.00
1204  4:R ZYG TP    150.21     86.57     0.00     0.00     0.00
1205  5:L ZYG TP    138.92     91.82     0.01     0.00     0.00
1206  6:R POSTMAN   127.58     45.61     0.01     0.00     0.00
1207  7:L POSTMAN   128.71     48.04     0.00     0.00     0.00
1208  8:R ANTMAN    153.73     23.76     0.01     0.00     0.00
1209  9:L ANTMAN    162.95     22.83     0.00     0.00    -0.00
  20 10:ANS         999.99    999.99
-------------------------------------------------------------------
1230 40:LL 6 APEX   999.99    999.99
-77
```

Dashes represent lines omitted in this example.

Average values for two tracings of the centered film of skull 1 series 1 lateral x-ray (last three columns measure the differences between tracings).

OFFSET AVEPIC FILE

```
8402     0.99091     3  8 84
01112    02/15/84    /  /      S. 1, SK 1
                        X          Y
 821 A :A FIDUCIA      0.00     -0.00      0.00      0.01      0.00
 822 B :B FIDUCIA    -10.85    178.27      0.00      0.00      0.00
 823 C :C FIDUCIA    210.54    189.96      0.00      0.00      0.00
 824 D :D FIDUCIA    242.00     -0.00      0.00      0.00     -0.00
1201  1:R SUPRCIL    118.29    135.33      0.01      0.01     -0.01
1202  2:L SUPRCIL    134.13    137.87      0.01      0.01     -0.01
1203  3:NASAL TP     134.89    110.92      0.01      0.01     -0.01
1204  4:R ZYG TP      92.50     83.62      0.01      0.00     -0.00
1205  5:L ZYG TP     113.67     90.52      0.01      0.00     -0.01
1206  6:R POSTMAN     73.97     42.79      0.01      0.00      0.01
1207  7:L POSTMAN     97.40     46.18      0.01      0.00     -0.00
1208  8:R ANTMAN     103.13     21.05      0.01      0.00      0.00
1209  9:L ANTMAN     125.66     20.84      0.01      0.01     -0.01
  20 10:ANS          999.99    999.99
-------------------------------------------------------------------
1230 40:LL 6 APEX    999.99    999.99
-77
```

Dashes represent lines omitted in this example.

Average values for two tracings of the offset film of skull 1 series 1 lateral x-ray (last columns measure the differences between tracings).

STEREO FILE

CENTERED 8402 1111 1112 021584 3/ 8/84
S. 1, SK 1 R SUPRCIL L SUPRCIL NASAL TP
1704.00 1684.00 64.04 93.19 1704.00 500.27 114.29 1684.00

	X	Y	Z				
A FIDUCIA	169.02	-85.14	195.12	-0.00	821	2	3
B FIDUCIA	178.29	87.49	150.00	-0.08	822	2	3
C FIDUCIA	179.12	29.33	-64.07	0.13	823	2	3
D FIDUCIA	169.98	-160.69	-34.74	-0.00	824	2	3
R SUPRCIL	0.00	0.00	0.00	-0.13	1201	2	3
L SUPRCIL	64.40	-0.00	-0.00	-0.18	1202	2	3
NASAL TP	31.36	-24.74	-0.00	-0.14	1203	2	3
R ZYG TP	-23.15	-36.97	31.07	-0.13	1204	2	3
L ZYG TP	81.78	-35.80	36.68	-0.07	1205	2	3
R POSTMAN	-12.48	-66.16	61.26	-0.14	1206	2	3
L POSTMAN	59.06	-70.46	58.98	-0.28	1207	2	3
R ANTMAN	-4.23	-92.86	45.01	-0.14	1208	2	3
L ANTMAN	38.10	-100.62	36.39	-0.10	1209	2	3
ANS	-999.90	-999.90	-999.90	0.00	20	2	3
LL 6 APEX	-999.90	-999.90	-999.90	0.00	1230	2	3

Dashes represent lines omitted in this example.

Three dimensional coordinate values derived from data on pages 69 and 70.

MERGE OUTPUT TO TERMINAL

THREE DIMENSIONAL CONFORMAL COORDINATE TRANSFORMATION

1ST FILE, 8402 1111, DEFINES COORD. SYSTEM

2ND FILE, 8402 1311, IS TRANSFORMED TO COORDS. OF 1ST FILE
& STORED AS =2000dig/200000418.3DM

SCALE FACTOR= 0.999221623 SIGMA HAT= 0.337 ITERATIONS= 6

ROTATION ANGLES	RADIANS	DEG	MIN	SEC	GRADS
OMEGA=	0.000853292	0	2	56	0.0543
PHI =	0.003736680	0	12	51	0.2379
KAPPA=	0.002886545	0	9	55	0.1838

ROTATION MATRIX

0.9999889135	0.0028897286	-0.0037341914
-0.0028865212	0.9999955297	0.0008640743
0.0037366713	-0.0008532859	0.9999927878

TRANSLATIONS

DX=	-0.543
DY=	-0.077
DZ=	0.158

RESIDUALS ON MERGE POINTS

	TRANSFORMED			FIXED		
POINT	VX	VY	VZ	VX	VY	VZ
R SUPRCIL	0.544	0.076	-0.156	-0.000	-0.000	0.000
L SUPRCIL	0.066	-0.110	0.085	-0.000	0.000	-0.000
NASAL TP	0.179	0.097	-0.060	-0.000	-0.000	0.000
R ZYG TP	-0.578	0.146	-0.108	0.000	-0.000	0.000
L ZYG TP	-0.211	-0.208	0.240	0.000	0.000	-0.000

COORDINATES FOR TRANSFORMED POINTS
IMAGE "S. 3, SK 1 " FIT TO "S. 1, SK 1 "

POINT	X	Y	Z	ID	
A FIDUCIA	-3.99	-3.15	1.36	821	FILE 2
A FIDUCIA	-0.00	0.00	0.00	821	FILE 1
A FIDUCIA	-3.99	-3.15	1.36	821	DIFF
A FIDUCIA	-1.99	-1.58	0.68	821	AVERAGE
B FIDUCIA	-7.01	-181.59	0.19	822	FILE 2
B FIDUCIA	-10.99	-178.32	-0.45	822	FILE 1
B FIDUCIA	3.98	-3.27	0.64	822	DIFF
B FIDUCIA	-9.00	-179.95	-0.13	822	AVERAGE
C FIDUCIA	214.70	-183.64	-0.15	823	FILE 2
C FIDUCIA	210.54	-189.90	-0.02	823	FILE 1
C FIDUCIA	4.16	6.26	-0.13	823	DIFF
C FIDUCIA	212.62	-186.77	-0.08	823	AVERAGE
D FIDUCIA	237.59	7.36	1.14	824	FILE 2
D FIDUCIA	241.96	0.01	-0.23	824	FILE 1
D FIDUCIA	-4.37	7.35	1.37	824	DIFF
D FIDUCIA	239.78	3.68	0.46	824	AVERAGE

Results of merging three dimensional coordinate data (like page 71) from lateral stereo pairs of series 1 and series 3.

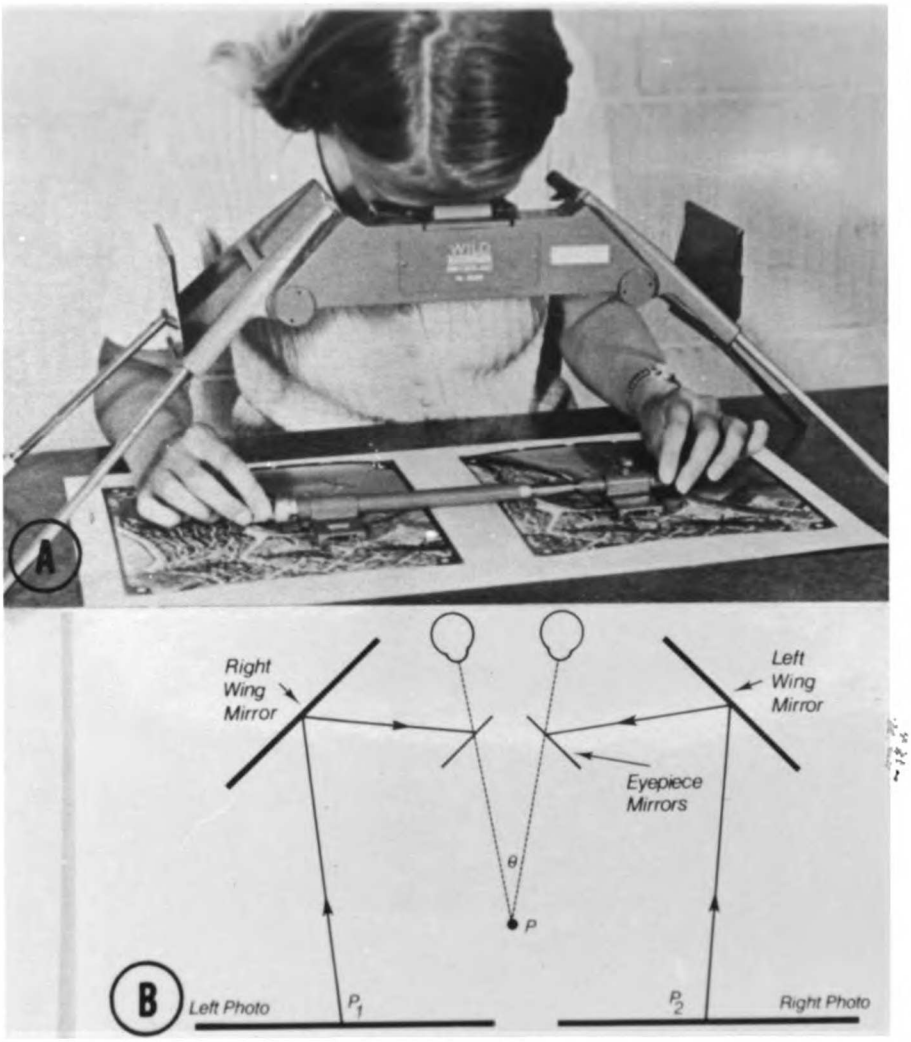

Fig. 1 Use of a mirror stereoscope and parallax bar in measuring the height of a point on a stereopair of aerial photographs. The principle of mirror stereoscope: When two stereophotographs are properly oriented on the surface below the instrument, information from each photograph is transmitted on only one eye. The two eyes and the brain merge the information from the two photographs and "perceive" a single three-dimensional virtual image in space. The heights of points within the virtual image can be measured with a parallax bar. (From Baumrind, S., et al. Am.J.Orthod. vol. 84:297, 1983; by permission.)

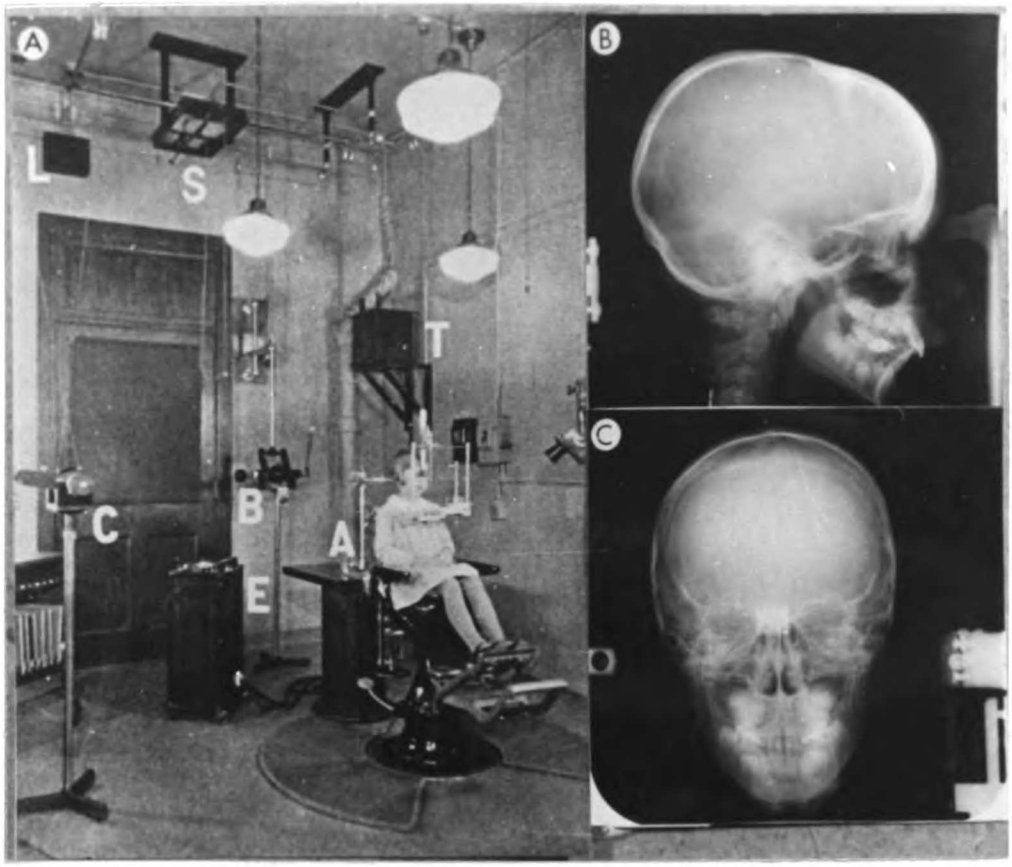

Fig. 2 A, The original Broadbent apparatus. (From Broadbent B.H..: Angle Orthod. 51:93, 1981.)
B and C, A representative Broadbent stereopair. (Courtesy of the Child Study Clinic Oregon Health Sciences University.)

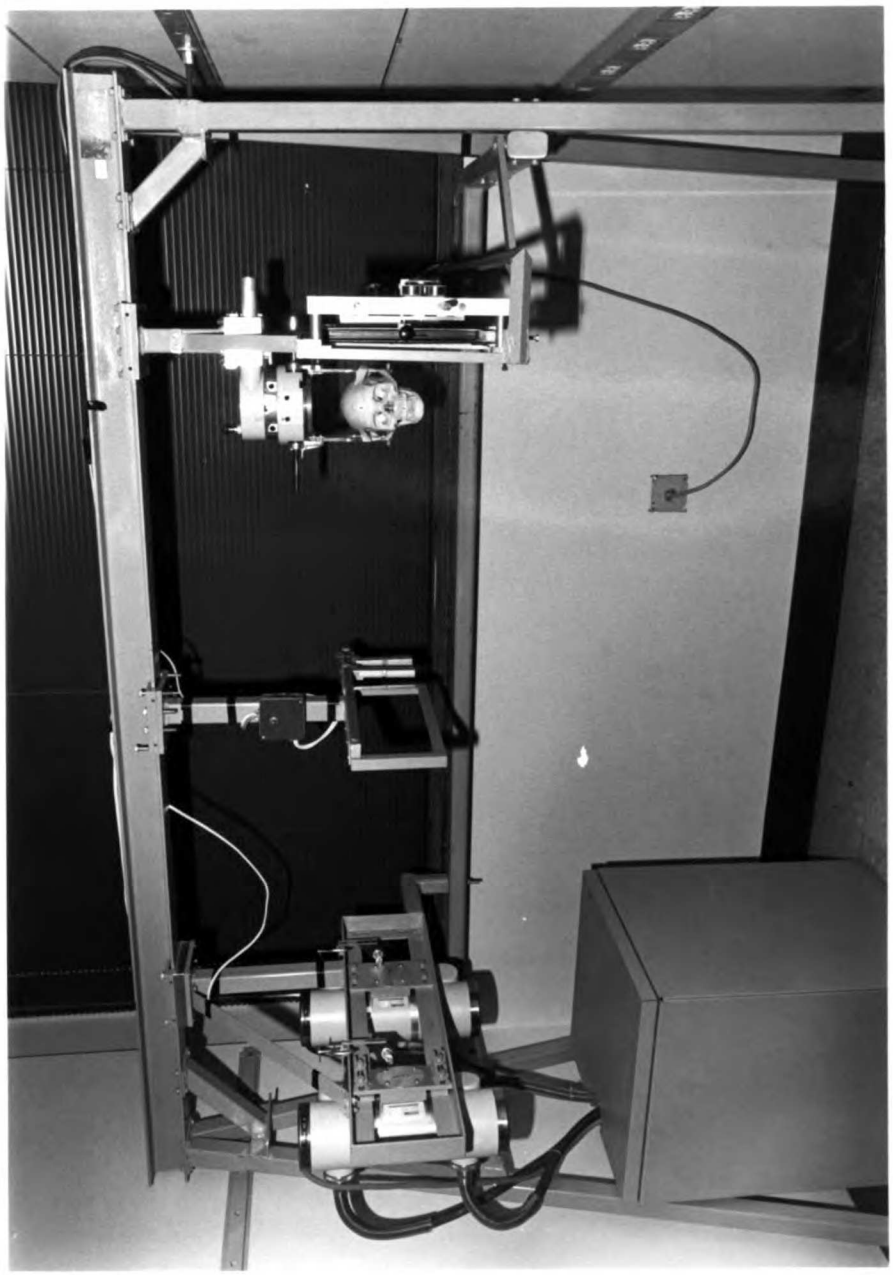

Fig. 3 General view of dedicated craniofacial stereometric x-ray system.

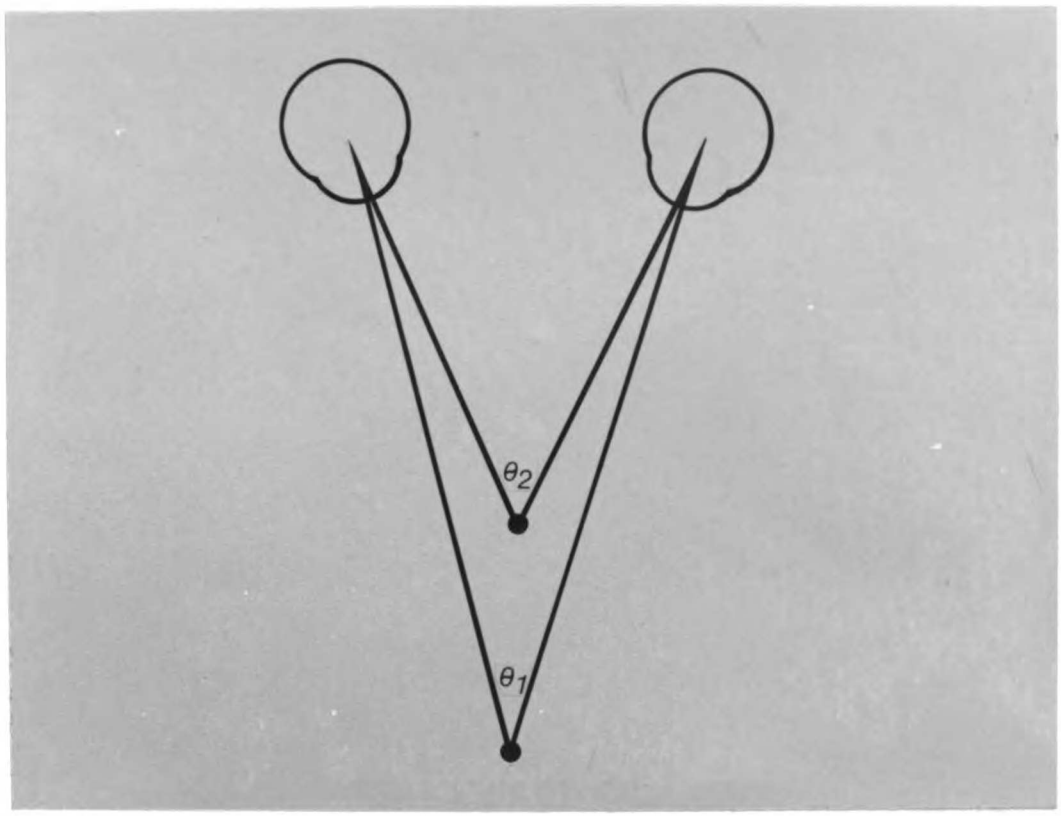

Fig. 4 The principle of stereoscopic distance perception. Points viewed at different distances will have different parallactic angles. These differences in paralactic angle are interpreted by the brain as differences in distance. (From Baumrind, S., et al.: Am.J.Orthod. vol 84:296, 1983; by permission)

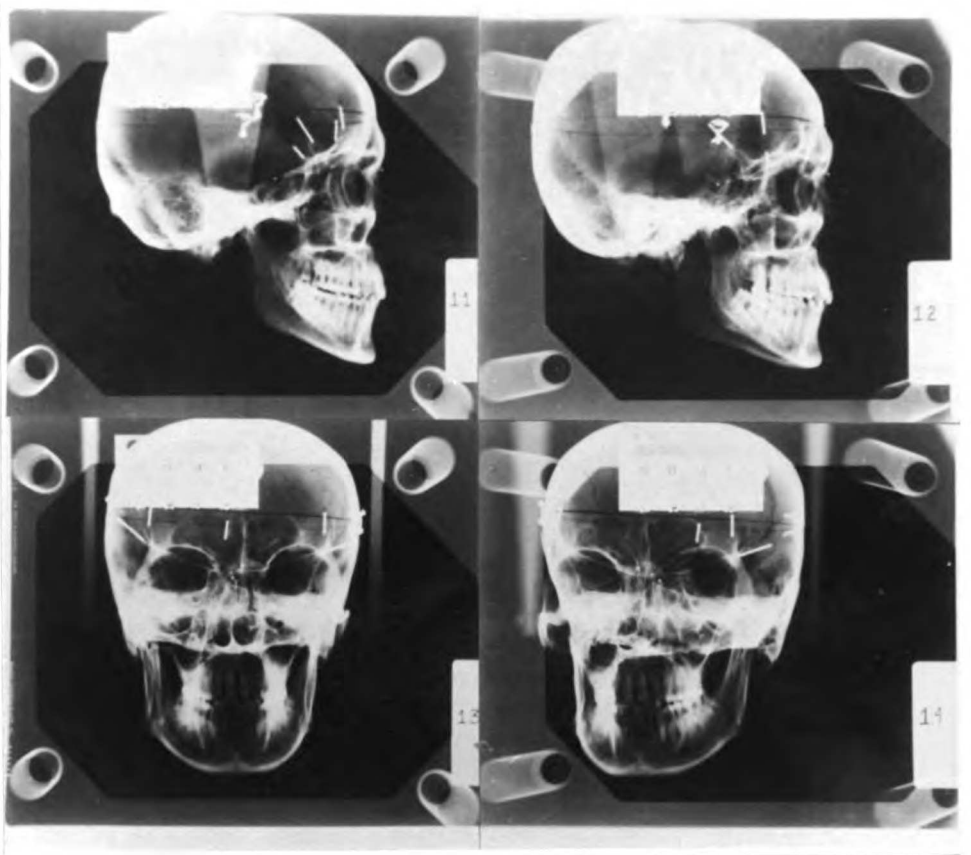

Fig. 5 Lateral and frontal stereopairs of dried skull. Upper row, left film: Norma lateralis projection. Upper row, right film: Oblique lateralis projection. Lower row, left film: Norma frontalis projection. Lower row, right film: Oblique frontalis projection. The upper row constitutes a lateral coplanar stereopair; the lower row constitutes a frontal coplanar stereopair; the left column constitutes a Broadbent stereopair. (From Baumrind, S., et al.: Am.J. Orthod. vol.84:301, 1983; by permission.)

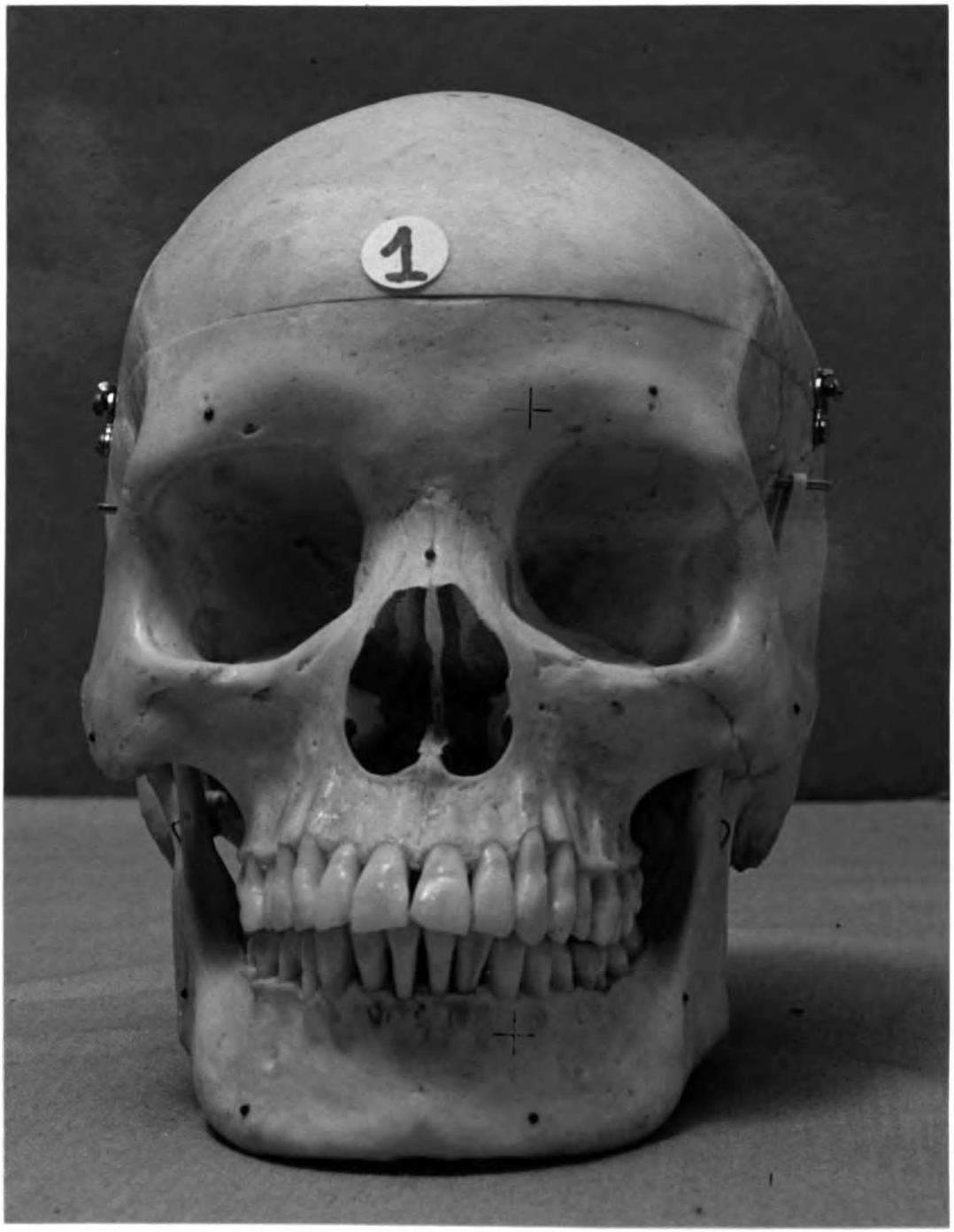

Fig. 6 Representative Skull, showing the nine reference markers (termed tie points) used as reference points within the skull for all subsequent series.

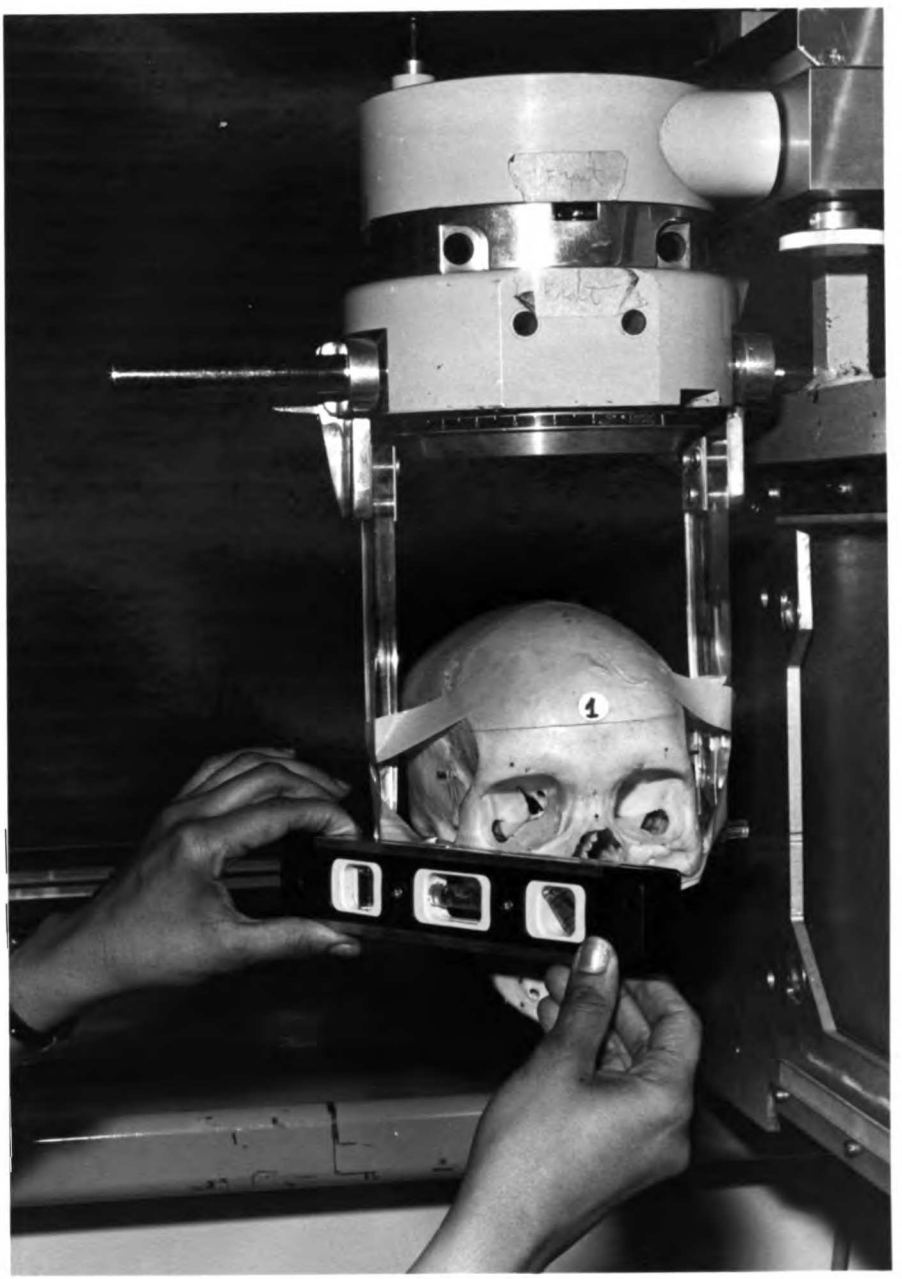

Fig. 7 Positioning of skull in the cephalostat. A carpenter's level is used to check the horizontal position of the Frankfort Plane.

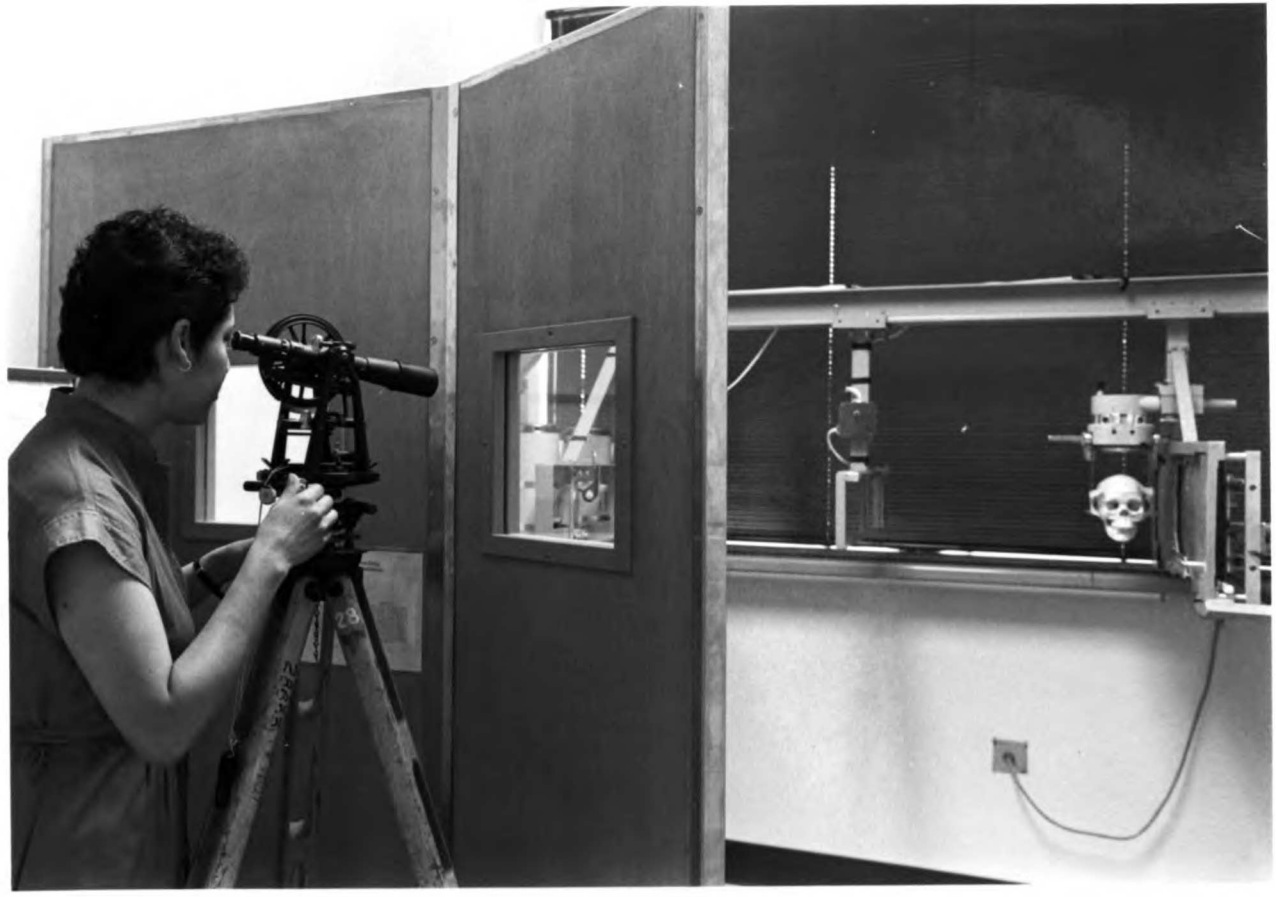

Fig. 8 Survey of a skull with the use of a theodolite.

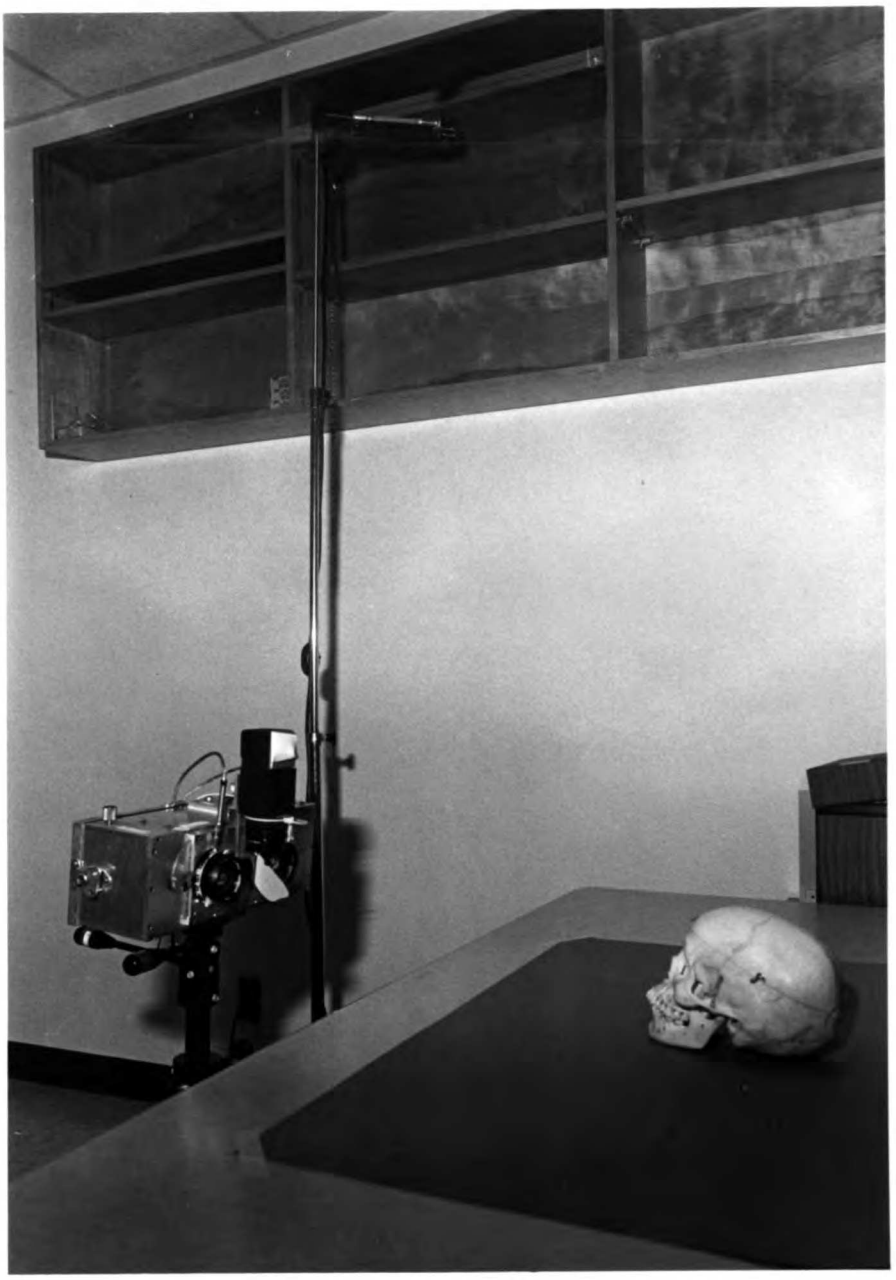

Fig. 9 Fully calibrated stereo camera used to take all stereo photographs of skulls.